Syndecan-1 and -4 influence Wnt signaling and cell migration in human breast cancers

Son H. Pham[1+], Kaylah Pratt[1+], Rachel K. Okolicsanyi[1], Lotta E. Oikari[1#], Chieh Yu[1^], Ian W. Peall[1], KM Taufiqul Arif[1], Te-Arn Chalmers[1], Martina Gyimesi[1], Lyn R Griffiths[1], Larisa M. Haupt[1,2,*]

[1]Queensland University of Technology (QUT), Centre for Genomics and Personalised Health, Genomics Research Centre, School of Biomedical Sciences, 60 Musk Ave., Kelvin Grove, Queensland 4059, Australia, [2]ARC Training Centre for Cell and Tissue Engineering Technologies, Queensland University of Technology (QUT), Australia

[+]Co-first authours

[#]Now located at: Cell and Molecular Biology, QIMR Berghofer Medical Research Institute, Queensland, Australia

[^]Now located at: Department of Cell and Tissue Biology, The University of California, San Francisco, USA

*Corresponding author:

Associate Professor Larisa M. Haupt

Genomics Research Centre

Queensland University of Technology

60 Musk Avenue, Kelvin Grove QLD 4059

Australia

E-mail: larisa.haupt@qut.edu.au

Abstract: Heparan sulfate proteoglycans (HSPGs) participate in numerous normal and pathophysiological cellular functions. HSPGs are crucial components of the extracellular matrix (ECM) binding signalling molecules such as fibroblast growth factors (FGF) and Wnts to mediate various cellular processes including cell proliferation, migration, and cancer invasion. The syndecans (SDCs1-4) are a major family of four HSPGs, implicated in the development of breast carcinomas. This study examined syndecan-1 (SDC1) and syndecan-4 (SDC4; SDC1/4) in breast cancer (BC) *in vitro* cell models and their role in tumorigenesis. Gene expression of HSPG core proteins, biosynthesis and modification enzymes along with Wnt/FGF morphogen pathway components were examined following inhibition of *SDC1* and *SDC4* via small interfering RNA (siRNA), and enhancement of HSPGs via addition of heparin and FGF. siRNAs knockdowns (KDs) were performed in the MCF-7 (lowly invasive and poorly metastatic) and the MDA-MB-231 (highly invasive and metastatic) human BC cell lines. Significantly decreased gene expression of *SDC1* and *SDC4* was observed in both cell lines following KD. Additionally, via gene expression analysis, downregulation of SDC1/4 decreased the biosynthesis of heparan sulfate modification enzymes and reduced expression of Wnt signalling molecules. Following the enhancement/inhibition of HSPGs via heparin/siRNA treatment, heparin increased the migratory characteristics of MCF-7 cells while KD of SDC1 increased cell migration in both MCF-7 and MDA-MB-231 cells when compared to scramble negative control conditions. Our findings suggest that a niche-specific function exists for SDC1/4 in the BC microenvironment, mediating Wnt signalling cascades and potentially regulating migration of BC cells.

Keywords: heparan sulfate proteoglycans, human breast cancer, MCF-7, MDA-MB-231, Wnt signalling, proliferation.

1. Introduction

Breast cancer (BC) is the most common type of cancer in women, with 1 in 7 Australian women diagnosed before the age of 85 [1]. BC is characterised by changes in microenvironmental components of the mammary gland, resulting in changes to cancer proliferation, migration and metastasis [2]. The extracellular matrix (ECM) defined as multi-component networks that surround cells in tissues, includes structures rich in proteins, including proteoglycans (PGs) decorated with glycosaminoglycans (GAGs), as well as the structural proteins collagen, and laminin [3]. The ECM contributes to the cancer microenvironment and contains a reservoir of cellular and non-cellular materials including proteoglycans (PGs) and growth factors (GFs) produced by both the epithelial and stromal cells [4, 5]. PGs are a major constituent of the ECM and exhibit important functions in normal biological processes, including cell development, apoptosis, cellular differentiation and in pathophysiological processes including cancer metastasis [6, 7]. Various studies have shown that PGs are altered during malignant transformation, although to what extent is yet to be fully elucidated [7, 8].

HSPGs are key members of the PG family and consist of a core protein with one or more covalently attached sulfated glycosaminoglycan (GAG) chains [9]. GAG chains contribute to and mediate a range of pathophysiological functions in normal and cancer cells through their binding of numerous extracellular ligands and morphogens [10]. The two major subgroups of HSPGs, the SDCs and glypicans (GPCs), are present on the mammalian cell surface with predominantly heparan sulfate (HS) side chains attached to the core protein [11]. SDC1 is a coreceptor for growth factors (GFs) and chemokines, and has been implicated in the process of epithelial-mesenchymal transition (EMT) during the development and increased tumourigenesis of BC [12]. SDC4 mediates the regulation of cell/cell adhesion, mortility, and cell proliferation, with the role of SDC4 in BC poorly understood [13]. While SDCs modulate cell proliferation, adhesion, migration and angiogenesis [13, 14], GPCs primarily modulate cell motility and morphogenesis [15]. HS side chains are initially produced in the Golgi but are subject to a complex temporal post-translational process mediated by various biosynthesis enzymes. SDCs are predominantly HS-related and thus depend on the structure of HS chains attached to the core protein. The combined action of the biosynthesis and modification HS enzymes determines the structure and role of these HSPGs [16]. This includes polymerisation by

exostosin glycosyltransferases (EXT1 and 2), C5 epimerisation by C5-epimerase (GCLE), heparan sulfate modification by N-deacetylase/N-sulfotransferases (NDST1 and NDST2), and O-sulfotransferases (HS 2-O-sulfation (HS2ST1) and HS 6-O-sulfation (HS6ST1)).

Therefore, any changes in the gene expression of these enzymes following SDC KDs may provide an assessment of an additional layer of regulation of the SDCs and provide some insight into any positive/negative feedback of the synthesis process. In addition, this complex and coordinated biosynthesis creates high structural and functional diversity making HSPGs key contributors of cell-cell and cell-matrix interactions due to their ability to bind various GFs and morphogens including FGFs, heparin-binding epidermal growth factor and other ECM cofactors [8, 17]. The intereactions between HSPGs and several morphogens including Wnts, FGFs and FGF receptors (such FGFR1) have been reported in several cancer cell types [18]. Wnt and FGF signalling pathways have been identified to regulate key cellular behaviours with the elevation of FGFR1 implicated in BC susceptibility [18].

The activation of Wnt signalling has been significantly associated with many cancers and to mediate self-renewal processes in both stem and cancer cells, enhancing malignant proliferation [19]. Wnt signalling is comprised of 3 pathways (canonical, noncanonical planar cell polarity and noncanonical Wnt/calcium) with the canonical Wnt pathway acting through β-catenin (CTNNB1) to regulate cell proliferation [8, 20]. In this study, gene expression of Wnt pathway genes (axis inhibitor protein 1/2 (*AXIN1/2), CTNNB1, FGFR1*), FGF receptors (*FGFR1*) and FGF morphogens (protein tyrosine kinase 2 (*PTK2*)), lymphoid enhancer-binding factor 1 (*LEF1*) and ras homolog family member A (*RhoA*) were examined in the MCF-7 and MDA-MB-231 human BC cell lines following inhibition of SDC1/4 via siRNA knockdown (KD). In addition, various PG biosynthesis enzymes, which provide key and microenvironmentally influenced modifications to HSPG side chains to mediate interactions with various signalling molecules including FGF and Wnt ligands [21] were also examined. A previous study has shown downregulation of the Wnt pathway is linked to EMT in BC [22]. Thus, the effect of HSPG SDCs on EMT via the Wnt pathway were examined to demonstrate the contribution of HSPG in regulating BC cell migration. EMT results in modulations in cytoskeletal organisation, focal adhesion and cancer tumorigenicity leading to increased metastasic potential [22]. Vimentin (VIM) and the Indian blood group protein (CD44) are well-established cancer stem cell

markers, highly associated with BC with increased VIM protein linked to a more invasive metastatic EMT phenotype [23, 24].

Establishing Wnt/FGF signalling pathway interactions with SDCs and various Wnt morphogens may reveal clinically relevant molecular targets for BC treatments. This study aimed to increase our knowledge of the contribution of SDCs within the BC microenvironment and to identify potential targets that limit or reduce tumour proliferation, invasion and migration and ultimately, lead to decreased severity of BC.

2. Materials and Methods

2.1 Cell Culture and Maintenance

The two human BC cell lines used in this study, MCF-7 and MDA-MB-231, were obtained from the American Type Culture Collection (ATCC) and expanded as monolayer cultures in Dulbecco's Modified Eagle (DMEM) medium containing 10% fetal bovine serum (FBS) and 100 U/mL penicillin/streptomycin. The MCF-7 and MDA-MB-231 cells were plated at 6-7 x 10^3 cell/cm^2 in T75 flasks and incubated at 37°C in a 5% CO_2 humidified atmosphere. Cells were maintained in the culture medium and passaged routinely at 70-85% confluence by removing the conditioned media, washing with 1 X phosphate buffered saline (PBS) and adding 5 mL of trypsin before incubation at 37°C for 5 min to dissociate the cell monolayer. The trypsin was then neutralised with 5 mL DMEM growth media. 10 µL of cell suspension was removed for determination of cell number and viability using the Trypan Blue exclusion method on a Bio-Rad TC20™ cell counter or haemocytometer. Media and supplements were obtained from Life Technologies, Australia unless otherwise stated. Plasticware was obtained from Corning, Australia unless otherwise stated.

2.2 Accell siRNA Transfection

Accell siRNA SMARTpool (Thermo Fisher Scientific, Australia) siRNAs (small interfering RNAs) were utilised to knockdown (KD) the gene expression of *SDC1* and *SDC4* in both MCF-7 and MDA-MB-231 cell cultures. siRNA KDs were performed following the manufacturer's protocols. Both cell lines were plated at 1 x 10^4 cells/well and grown until 60-70% confluence prior to Accell siRNA transfection. Each KD experiment generated triplicate RNA and protein samples, which were pooled at completion of the assay and prior to subsequent analysis. The sample groups included: untreated cells (UT), negative control siRNA (Accell non-specific targeting siRNA – scramble; SCR), *SDC1* knockdown (*SDC1* siRNA; SDC1KD) and *SDC4* knockdown (*SDC4* siRNA; SDC4KD). As no statistical difference between the untreated and scramble conditions were observed, the data from these conditions were combined to create a control condition for comparison to KD groups in Q-PCR experiments. siRNAs were used at a working concentration of 1 µM and incubated with the cells at 37°C in 5% CO_2 without media change for 72 h for RNA and 96 h for

protein isolation. The KD efficiency of target genes was assessed (**Figure 1**) and as in our previous studies demonstrated that KD provided significant downregulation of target genes with no effect on viability of the cells [25, 26]. All siRNA sequences utilised can be found in **Supplementary Table 1**.

2.3 RNA Isolation and Reverse Transcription

Following siRNA gene KDs of *SDC1* and *SDC4*, delivery media was removed and cells washed with 1 X PBS. Both MCF-7 and MDA-MB-231 cell lines were trypsinised with 100 µL trypsin/well and cells allowed to dissociate prior to neutralisation with 100 µL DMEM. Each well in a 24-well plate was washed with 1 X PBS and all replicates were pooled before calculating cell number using a haemocytometer. Cells were centrifuged at 3 000 x g for 5 min, the supernatant was discarded, and the pellet resuspended in 1 X PBS prior to being centrifuged at 5 000 x g for 5 min. The supernatant was then discarded and the pellet resuspended in 300 µL of TRIzol (Invitrogen) and stored at -80°C for at least 24 h prior to RNA extraction. The RNA was isolated using a Direct-zol RNA MiniPrep Kit (Zymo Research Corp., USA) following the manufacturer's instructions. The purity and concentration of the extracted RNA was assessed using a NanoDrop 8000 spectrophotometer (Thermo Scientific, Australia).

Roche transcriptor reverse transcriptase or BioRad iScript™ Reverse Transcription kits were utilised to convert RNA to cDNA. For the Roche transcriptor reverse transcriptase kit, 150 ng of RNA was incubated with 300 ng of Random Hexamer Primers (Invitrogen) in a total reaction volume of 20 µL for 10 min at 65°C and 5 min at 4°C. After incubation, 20 U of RNaseOUT (Invitrogen), 1 mM dNTPs (BioLab) and 10 U of Transcriptor Reverse Transcriptase (Roche) was added, resulting in a final volume of 30 µL in 1 X Reverse Transcriptase buffer (Roche). This was incubated at 25°C for 10 min then 55°C for 30 min and finally 85°C for 5 min. For the BioRad iScript™ Reverse Transcription kit, 150 ng of RNA was added into 4 µL of 5 X iScript reaction mix, 1 µL of iScript reverse transcriptase and Nuclease-free water in a total reaction volume of 20 µL for 5 min at 25°C then 20 min at 46°C and finally 1 min at 95°C. The resulting cDNA was assessed for purity and concentration using the NanoDrop 8000 spectrophotometer (Thermo Fisher Scientific, Australia) then dilution in RNAase Free H_2O to a working concentration of 40 ng/µL with no

differences observed between the two methods.

2.4 Quantitative real-time polymerase chain reaction (Q-PCR)

Changes in gene expression of HSPG biosynthesis and modification enzymes, core proteins and both the canonical and non-canonical FGF/Wnt pathways members were then examined in the MCF-7 and MDA-MB-231 BC cell lines. Q-PCR was used to analyse the KD efficiency of *SDC1* and *SDC4* KDs in both cell lines. All Q-PCRs were performed using the QuantStudio 7 Flex Real-Time PCR system (Life Technologies) on 384-well plates with each sample run in technical quadruplicate. Amplification of 120 ng of cDNA was undertaken in a 10 µL reaction containing 1X SYBR Green PCR Master Mix (Promega), 200 ng each of forward and reverse primer and 0.1 µL 1X CXR reference dye (Promega). Samples were amplified using thermocycling conditions (50°C for 2 min, 95°C for 3 min, 50 cycles of 95°C for 3 sec and 60°C for 30 sec) and gene expression was normalised against *18S* gene expression (endogenous control) using the $2^{-\Delta\Delta Ct}$ method as previously [8, 26]. Data is presented as the fold change between the control and KD conditions with error bars representing Standard Deviation (SD). All primer sequences for the genes analysed can be found in **supplementary Table 2**.

2.5 Immunocytochemistry (ICC)

KD of *SDC1* and *SDC4* genes were completed using Accell siRNA SMARTpool (Thermo Fisher Scientific) siRNA following manufacturer's instructions in MCF-7 and MDA-MB-231 cell cultures. MCF-7 and MDA-MB-231 cells were plated at 3 x 10^3 cells/well in 24-well plates to prevent cells reaching overconfluence and allowed to attach for 24 h prior to siRNA transfection. Following addition of siRNAs, cells were incubated for 96 h before the culture medium was removed, cells were then fixed with 4% paraformaldehyde (PFA) in 1X PBS for 30 min at room temperature and rinsed three times with 1X PBS. Cells were then incubated in blocking solution containing: 1% Bovine Serum Albumin (BSA) and 2% normal donkey serum in 1X PBS for 2 h at room temperature. Next, primary antibodies diluted in blocking solution were added and incubated at 4°C overnight. The primary antibodies and dilutions used were: anti-SCD1 (1:200; ab34164, Abcam), anti-SDC4 (1:1 000; ab24511, Abcam), anti-vimentin (1:200; ab8069, Abcam), and anti-CD44 (1:200; ab6124, Abcam). Following overnight incubation with primary antibodies,

MCF-7 and MDA-MB-231 cells were washed three times with 1X PBS followed by incubation with secondary antibodies, FITC-conjugated donkey anti-mouse IgG (1:1 000; AP192F, Sigma-Aldrich) and Cy3-conjugated donkey anti-rabbit IgG (1:1 000; AP182C, Sigma-Aldrich) diluted in blocking solution for 2 h at room temperature. MCF-7 and MDA-MB-231 cells were then rinsed three times with 1X PBS, and cells incubated with DAPI for nuclear counterstaining (Molecular ProbesTM) for 15 min at room temperature. Cells were then mounted with ProLong™ Diamond Antifade Mountant without DAPI mounting medium (P36961, Thermo Firsher, Australia). Images of the MCF-7 and MDA-MB-231 cells were taken on an Olympus IX81 inverted phase-contrast fluorescent microscope using Volocity software v6.3 (Quorum Technologies, Canada). For ICC images, the signal intensity was analysed by normalising the mean signalling of examined protein and dividing it by the number of nuclei obtained using Volocity software v6.3.

2.6 Western Blotting

Following siRNA gene KDs, Accell siRNA delivery media was removed from the MCF-7 and MDA-MB-231 cultures and the cells washed with 1X PBS. The MCF-7 and MDA-MB-231 cells were then dissociated from the monolayer using trypsin and neutralised with DMEM +10% FBS. Cell counting and viability analysis was undertaken with 10 µL of cell suspension using Trypan Blue exclusion on a Bio-Rad TC20^{TM} cell counter. The 24-well plate wells containing MCF-7 or MDA-MB-231 cells were then washed with 100 µL of 1X PBS and all replicates were pooled. Pooled cell suspensions were the centrifuged at 3 000 x g for 5 min, the supernatant discarded, and the pellet resuspended in 1X PBS and re-centrifuged at 5 000 x g for 5 min. Total protein was extracted using 100 µL RUNX protein lysis buffer (20 mM 4-(2-hydroxyethyl)-1-piperazineethanesulfonic acid (HEPES), 25% glycerol, 420 mM NaCl, 1.5 mM $MgCl_2$, 0.5 mM DTT, 0.2 mM EDTA, 0.5% IGEPAL CA-630, 0.2 mM sodium orthovanadate (Na_3VO_4), 1 mM PMSF in dH_2O containing protease and phosphatase inhibitors at 1:100) per sample. For protein lysis, samples were vortexed before sonication and further centrifuged at 14 000 x g for 20 min at 4°C.

The bicinchoninic acid (BCA) protein quantitation assay (Pierce, Australia) was then used for protein determination. Approximately 30 µg of total protein in 6 X loading dye was separated by sodium dodecyl sulfate - polyacrylamide gel electrophoresis (SDS-PAGE) using 10% Ammonium

persulfate solution (APS) on 1.0 mm mini gels (TGX Stain-Free FastCast, Bio-Rad). Gels were run constantly at 150 V for 1 h. Following separation, the protein was transferred to 0.2 mm Polyvinylidene fluoride (PVDF) membranes using the Bio-Rad Transblot Turbo System at 1.0 A and 25 V for 30 min. After transfer, the membrane was blocked with 5% milk/1X Tris-Buffered Saline (TBS), and washed three times with 1X 0.1% Tween® 20 Detergent in TBS (TBST) before primary antibodies diluted in 5% bovine serum albumin (BSA)/TBST were added and incubated overnight at 4°C. Primary antibodies used were: anti-vimentin (1:1 000; ab8069, Abcam) and anti-CD44 (1:500; ab6124, Abcam). The PVDF membranes were then washed three times with 1X PBS before incubation with horseradish peroxidase (HRP)-conjugated secondary antibodies; anti-Mouse IgG (#7076, Cell Signalling) at a dilution of 1:1 000 and anti-Rabbit IgG (#7074, Cell Signalling) at a dilution of 1:3 000 in 5% BSA for 2 h at room temperature. Enhanced chemiluminescence (ECL) (Clarity^{TM} ECL, Bio-Rad) reagent was used to detect target proteins using the Fusion FX Spectra chemiluminescence settings (Vilber Lourmat, Fisher Biotec).

2.7 Scratch Assay

The MCF-7 and MDA-MB-231 cells were plated at 2 x 10^5 cells/well in 6-well plates and allowed to attach and synchronise overnight using low serum growth media (2% FBS). For the HSPG enhancement conditions, heparin (10 µg/mL) or FGF-2 10ηg/mL were added to the cell cultures in 2% FBS or 10% FBS to group samples as 2% FBS, 2%FBS heparin (10 µg/mL), 2% FGF-2 (10ηg/mL), 10% FBS, 10% FBS + FGF-2 (10ηg/mL), 10% FBS + heparin (10 µg/mL). For KD cultures, the *SDC1* and *SDC4* genes were silenced using Accell siRNA SMARTpool (Thermo Fisher Scientific) siRNA following manufacturer's instructions in both BC cultures with MCF-7 and MDA-MB-231 cells plated in 2 mL of 1 µM siRNA delivery media (DharmaconTM Acell siRNA, GE Healthcare) per well. The sample groups were: UT, SCR, SDC1KD and SDC4KD.

Each well was scratched horizontally using a p200 pipette tip and a ruler through the center as previously described [27]. The MCF-7 and MDA-MB-231 cells were then incubated at 37ºC with 5% CO_2, without media change and observed over a 72 h period. Images of the scratch were taken on an Olympus IX81 inverted phase-contrast microscope using Volocity software v6.3 and v6.5 (Quorum Technologies, Canada) at 0, 12h, 24h, 48h and 72h timepoints. Triplicate measurements were taken at each of 3 fields of view across the scratch. Measurments at 4X magnification of scratch

width were made and analysed using the Quantitation module of Volocity v6.3 and v6.5. Following completion of the scratch assay cells were harvested for RNA as previously described.

2.8 Statistical analysis

Each gene expression experiment was perfomed in biological triplicate and technical quatruplicate (n=4). cDNA collected from UT and SCR conditions were combined to create a control condition for comparison to KD groups. The results are presented as target gene expression level as fold change ± standard deviation (SD). *P* values were calculated by student's *t* test for gene expression, and one way ANOVA test for ICC signal intensity, with a value of $p < 0.05$ considered as significant. Significant differences were visualised and presented using GraphPad Prism 8.4.3 in the relevant figures.

3. Results

3.1 SDC1 and SDC4 KD mediates HSPG core protein gene and protein expression

Following SDC1/4 KD, significant decreases in gene expression of *SDC1* and *SDC4* in both MCF-7 and MDA-MB-231 cell lines was observed (**Figure 1A & B**). *SDC1* gene expression was significantly downregulated in SDC1KD cultures (MCF-7: 51% with $p = 0.0424$, MDA-MB-231: 50% with $p = 0.0067$) when compared to controls. Gene expression of *SDC4* was significantly decreased post SDC4KD (MCF7: 75% with $p = 0.0456$, MDA-MB-231: 44% with $p = 0.0014$) when compared to control conditions. This high KD efficiency of the SDC1KD and SDC4KD on target gene expression also resulted in significant changes in other HSPG core proteins in both MCF-7 and MDA-MB-231 cells.

In MCF-7 cells, SDC1KD significantly decreased gene expression of *SDC4* (76% with $p = 0.0432$), but non-significantly dereased the gene expression of *SDC2* and *SDC3* when compared to control conditions (**Figure 1C**). SDC4KD significantly downregulated the gene expression of *SDC1* (79% with $p = 0.0074$), *SDC2* (73% with $p = 0.0248$), and non-significantly increased gene expression of *SDC3* when compared to control conditions. (**Figure 1C)**. In MCF-7 cultures, SDC1KD and SDC4KD did not appear to affect *GPC1* and *GPC4* gene expression (**Figure 1D**). Basal *GPC5* gene expression was not expressed in MCF-7 cells (data not shown), *GPC6* gene

expression was significantly decreased following KD of both SDCs (SDC1KD: 46% with p = 0.0408; SDC4KD: 73% with p = 0.0058) (**Figure 1D**).

In MDA-MB-231 cells, SDC1KD decreased gene expression of *SDC4* (p = 1.1755E-05), with SDC4KD significantly decreasing *SDC1* gene expression (52% with p = 0.0247) when compared to control conditions (**Figure 1E**). *SDC2/3* gene expression was not affected by KD of SDC1/4. Similar to MCF-7 cultures, *GPC1* gene expression was significantly downregulated in SDC1KD (76% with p = 5.0572E-05) in MDA-MB-231 cells. Interestingly, basal *GPC4* gene expression was not detected in MDA-MB-231 cells in all culture conditions. *GPC5* gene expression was significantly decreased after SDC1KD (14% with p = 0.0238), and GPC6 gene expression was not affected by KD of SDC1/4 MDA-MB-231 cultures (**Figure 1F).** The lack of basal GPC4/5 expression in the MCF-7 and MDA-MB-231 cells respectively in the KD delivery media, is consistant with previous studies (Okolicsanyi *et al.* 2014).

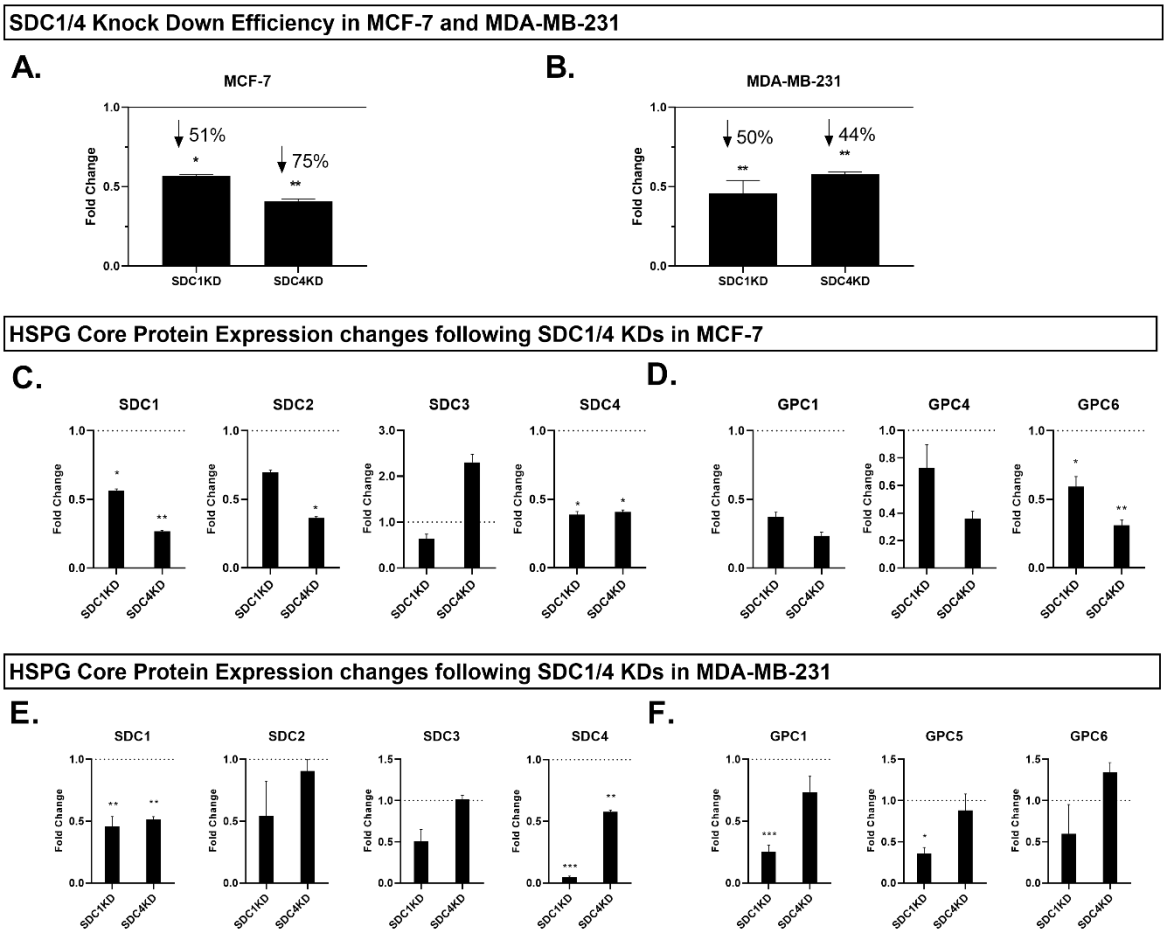

Figure 1. *The efficiency of heparan sulfate proteoglycan (HSPG) downregulation of syndecan (SDC) SDC1 and SDC4 genes following targeted siRNA knockdown (KD) (A) KD efficiency of SDC1 and SDC4 in basal MCF-7 and (B) the MDA-MB-231 cultures. The KD efficiency was examined by gene expression of SDC1 and SDC4 in SDC1KD and SDC4KD was compared to control conditions respectively. KD of SDCs resulted in significantly decreased gene expression of SDC1 (MCF-7: 51% with p = 0.0424, MDA-MB-231: 51% with p = 0.0067) and SDC4 (MCF7: 75% with p = 0.0456, MDA-MB-231: 44% with p = 0.0014) in both cell lines suggesting the gene specific siRNAs provide high efficiency in silencing the target HSPG core proteins. HSPG core protein gene expression profile of (A) MCF-7 and (B) MDA-MB-231 cells following SDC1 and SDC4 siRNA KDs. The untreated and scrambled conditions were combined to form the control condition to which gene expression was normalised. Each gene expression experiment was perfomed in biological triplicate and technical quatruplicate (n=4). Relative gene expression in MCF-7 cells of (C) SDC1-4 (D) glypican (GPC) GPC1,-4 and -6; and in MDA-MB-231 cells of (E) SDC1-4, (F) GPC1,-5 and -6. The control mean is represented by the dotted line and is set to 1.0 fold change with the standard deviation of the experimental groups represented by the error bars. P values were determined using Student t-Test with significance denoted by *p<0.05, **p<0.01, ***p <0.001.*

SDC1 and SDC4 protein expression was also examined in both SDC1/4 KD cultures via ICC to validate gene expression results as well as to detect cellular localisation. SDC1 protein expression was significantly decreased in SDC1KD cultures when compared to negative control (scrambled, SCR) conditions in MCF-7: (p = 3.1288E-08), and compared to UT in MDA-MB-231 (p = 0.0008) (**Figure 2A & B**). SDC1 protein expression was also significantly decreased in SDC4KD when compared to SCR in both cell lines (MCF-7: p =8.5285E-07, MDA-MB-231: p = 0.0037) and when compared to UT in MDA-MB-231 cells (p = 1.5000E-06) (**Figure 2A**).

The ICC signal intensity was quantitated to normalised to the control (UT/SCR) condition that SDC4 protein expression was found to be downregulated in SDC1KD cultures when compared to UT cultures (p = 3.5802E-11) in MCF-7 cells, and compared to SCR MDA-MB-231 cells (p = 0.0070). The level of SDC4 protein was significantly downregulated post SDC4KD when compared to the control cultures in both cell lines, in MCF-7 cells, UT: p = 6.1356E-05, SCR: p = 1.3763E-10; and MDA-MB-231cells, UT: p = 0.0002 (**Figure 2 A & B**). Interestingly, specific gene siRNAs were used to KD SDC1/4 at the mRNA level. Due to the type of inhibition and the time points used, it is feasible that subsequent protein KDs may not be as efficient. In addition, there is also a delayed response to gene KD at the protein level. In many cases, this delay is 24 h following mRNA knockdown, which is why the 96 h timepoint was included. However, the change in protein levels may be further delayed in these cultures with a complete protein response not observed.

ICC examination showed both SDC1 and SDC4 proteins localised to the cell surface in cultures, with these patterns distinct from one another. Localisation of the SDC1 protein appeared to be more ubiquitous throughout the cell and to be more diffuse in the MCF-7 cultures when compared with MDA-MB-231 cell cultures. In comparison, SDC4 protein was shown to be localised around the nucleus in cluster like formations with SDC4 levels appearing to be lower in MCF-7 cultures when compared to MDA-MB-231 cells in all conditions examined (**Figure 2**). The ICC images supported the Q-PCR data that KD of the target genes decreased protein expression of SDC1/4 when compared to SCR/UT conditions in both MCF-7 and MDA-MB-231 cell cultures.

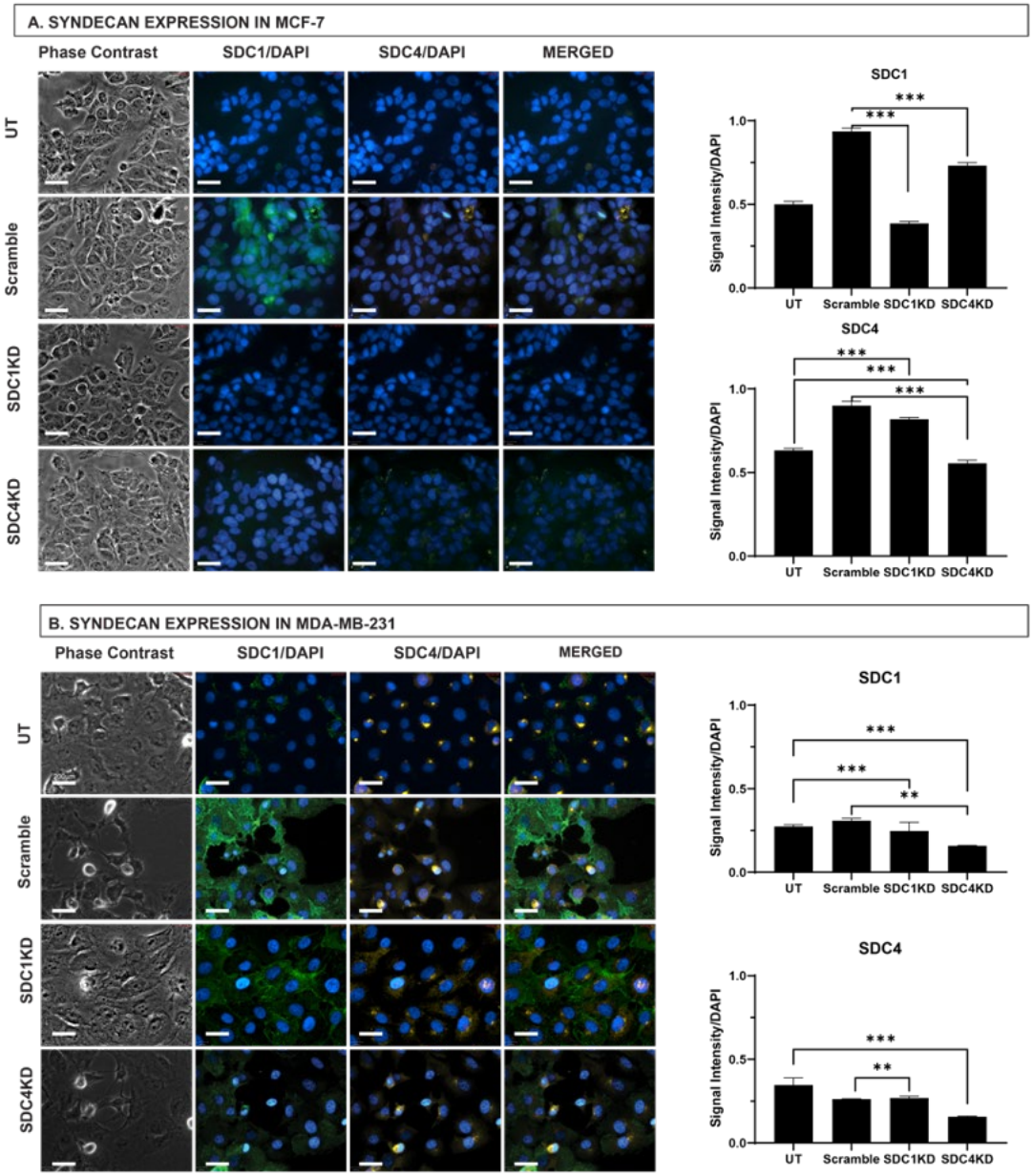

Figure 2. *Immunocytochemistry (ICC) of syndecan (SDC) SDC1 and SDC4 following SDC1/4 siRNA KD: SDC1 (FITC/green) and SDC4 (Cy3/yellow) detected at 96 h time point in (A) MCF-7 and (B) MDA-MB-231 cells– counterstained with DAPI (blue; 40X magnification, scale bar 200 μm). Immunofluorescence signal intensity of SDCs as measured by Volocity Cellular Imaging & Analysis software (Quorum Technologies, Canada) normalised to the signal intensity of DAPI. SDC1 and SDC4 protein expression was found to be higher in MDA-MB-231 cells when compared to MCF-7 cells with distinctly different localisation patterns: SDC1 localisation was more ubiquitous throughout the MDA-MB-231 cells while SDC4 localised around the nucleus in cluster formations. The SDC knockdown (KD) SDC1KD and SDC4KD conditions showed reduced protein expression of SDC1 and SDC4 in both MCF-7 and MDA-MB-231 cells compared to controls (untreated and scramble). ICC signal intensity differences were determined by ANOVA with significance denoted by *p<0.05, **p<0.01, ***p <0.001.*

3.2 SDC1 and SDC4 KD significantly alters HS biosynthesis and modification enzyme gene expression

The gene expression levels of a number of HS side chain biosynthesis and modification enzymes were then examined in both MCF-7 and MDA-MB-231 cells following siRNA KD of *SDC1* and *SDC4*.

In MCF-7 cells, SDC1/4 KD did not affect the gene expression level of HS chain initiation and polymerisation enzymes *EXT1 and EXT2* (**Figure 3A**). *GCLE* gene expression was increased following SDC1KD (p = 0.0064) in MCF-7 cultures (**Figure 3B**). The gene expression of the modification enzymes *NDST1* and *NDST2 (*N-deacetylase/N-sulfotransferases) was decreased following SDC4KD (NDST1: p = 0.0374; NDST2: p = 0.0338). SDC1KD induced a significant decrease of *NDST2* gene expression (p = 0.0272) when compared to the control in MCF-7 cells (**Figure 3C**). Modifications of HS chains include *O*-sulfation catalysed by *HS2ST1* and *HS6ST1*. *HS2ST1* gene expression was significantly downregulated post SDC4KD (p = 0.0451) in MCF-7 cells. *HS6ST1* gene expression was decreased significantly following both SDC1KD (p = 0.0365) and SDC4KD (p = 0.0367) in MCF-7 cells (**Figure 3D**).

In MDA-MB-231 cultures, SDC1KD also significantly reduced *EXT1* (p = 0.0048), *EXT2* (p = 0.0006) and *GCLE* (p = 0.0003) gene expression when compared to control cultures (**Figure 3E & F**). *EXT1* gene expression was also significantly increased in SDC4KD (p = 0.0002) cultures in MDA-MB-231 cells. *EXT2* gene expression remained unchanged in the MDA-MB-231 cells. *GCLE* gene expression was significantly decreased after SDC1KD (p = 0.0003) in MDA-MB-231 cultures

(**Figure 3F**). For the modification enzymes, *NDST1* gene expression was significantly increased after SDC4KD ($p = 0.0175$) in MDA-MB-231 cells, while *NDST2* gene expression significantly decreased after SDC1KD ($p = 0.0014$) (**Figure 3G**). *HS2ST1* gene expression was significantly downregulated following SDC1KD ($p = 0.0006$) in MDA-MB-231 cultures, while SDC4KD ($p = 2.1572E-05$) resulted in a significant increase in *HS2ST1* gene expression. In contrast to MCF-7 cells, a significant decrease in gene expression of *HS6ST1* was observed in SDC1KD ($p = 0.0116$) in MDA-MB-231 cultures (**Figure 3H**). These results demonstrate significant gene expression changes in HSPG biosynthesis and modification enzymes after the SDC gene-specific KDs in both MCF-7 and MDA-MB-231 cell lines reflecting the changing microenvironment and cell behavious within the cultures.

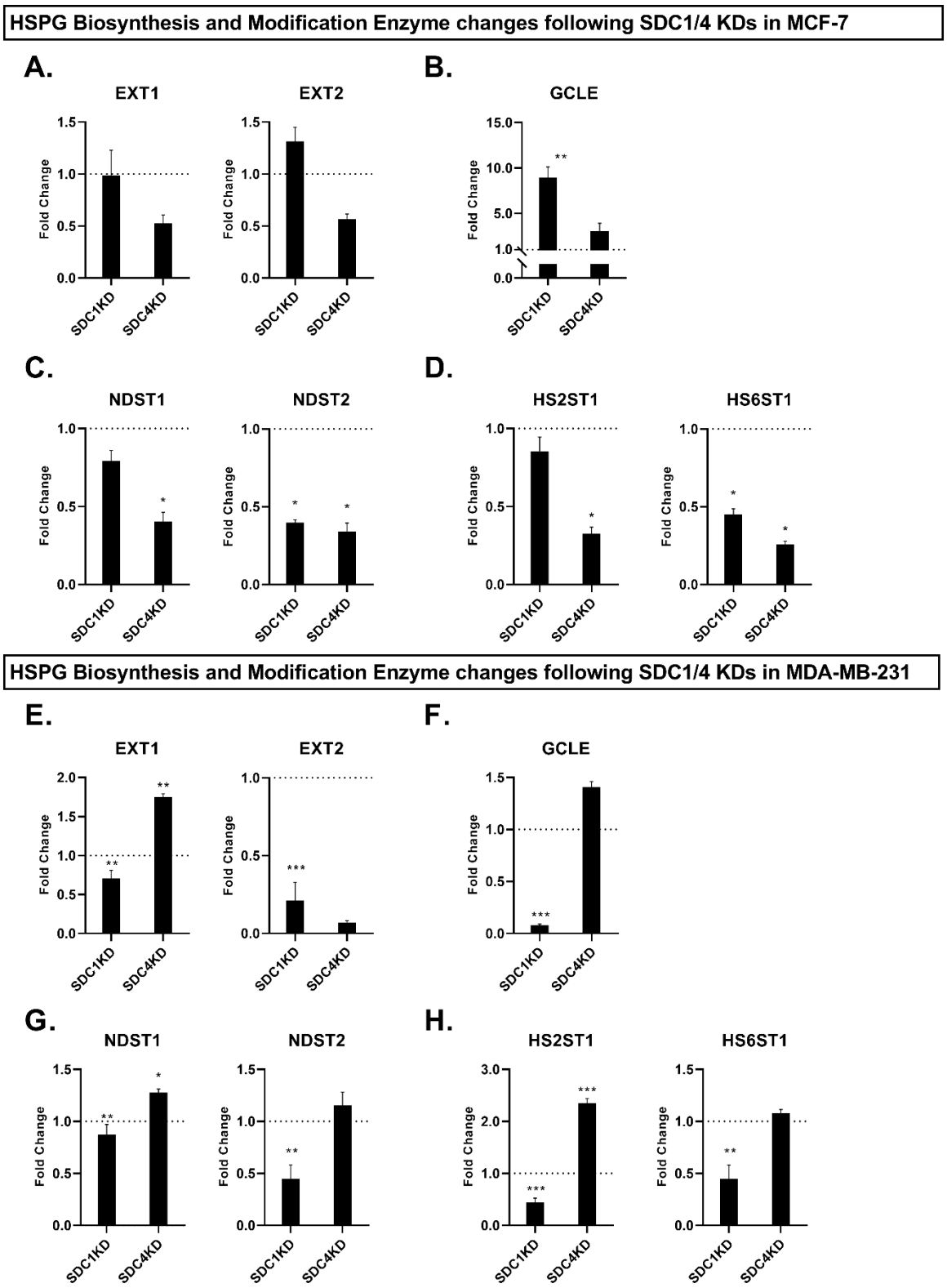

Figure 3. *Relative Gene Expression of heparan sulfate (HS) chain initiation and modification enzymes following* syndecan (SDC) *SDC1 and SDC4 siRNA knockdown (KD) in MCF-7 and MDA-MB-231 BC cell lines: MCF-7 cultures: (A) Exostoses (EXT1 & 2), (B) C5-Epimerase (GCLE), (C) N-deacetylase/N-sulfotransferases (NDST1 & NDST2), (D) 2-O/6-O-sulfotransferases (HS2ST2 & HS6ST1); and MDA-MB-231 cultures: (E) EXT1 & 2, (F) GCLE, (G) NDST1 & NDST2, (H) HS2ST2 & HS6ST1. SDC1/4 KD induced significant changes in the gene expression*

*of HS chain initiation and modification enzymes in both cell lines. The mean level of expression in control cultures is represented by the dotted line and set to 1.0 fold change with the standard deviation of the experimental groups indicated by error bars. Each gene expression experiment was perfomed in biological triplicate and technical quatruplicate (n=4). P values were determined using a Student's t-Test with significance denoted by *p<0.05, **p<0.01, ***p <0.001.*

3.3 SDC1 and SDC4 KD alters Wnt/FGF signalling pathway gene expression

KD of SDC1/4 also resulted in significant changes in gene expression of Wnt and FGF signalling pathway genes in both MCF-7 and MDA-MB-231 cell lines. In MCF-7 cells, examination of Wnt signalling morphogens, identified that the gene expression of *AXIN1* was non-significantly increased following SDC1KD, and non-significantly decreased in SDC4KD cultures when compared to controls (**Figure 4A**). *AXIN2* gene expression showed significant downregulation after SDC1KD (p = 0.0048) and SDC4KD (p = 0.0085). *CTNNB1* gene expression was non-significantly increased in both SDC KD cultures when compared to control MCF-7 cultures. *FGFR1* gene expression was also found to be non-significantly changed after both KD conditions when compared to control conditions in MCF-7 cells (**Figure 4A**). *LEF1* gene expression was shown to be non-significantly decreased in SDC1KD, with both *PTK2* and *RhoA* gene expression were found to be significantly downregulated following SDC1KD (*PTK2:* p = 0.0242; *RhoA:* p = 0.0377) and SDC4KD (*PTK2:* p = 0.0353; *RhoA:* p = 0.0109) when compared to control conditions in MCF-7 cultures (**Figure 4B**). In summary, gene expression of the Wnt signalling morphogens examined was not consistently altered (up/down regulated) following SDC1/4 KD in MCF-7 cultures.

In MDA-MB-231 cells, examination of the gene expression of the Wnt signalling morphogens identified a non-significant downregulation of *AXIN1* gene expression in both SDC KD conditions when compared to control. Interestingly, SDC1KD also induced a downregulation in both Wnt and FGF signalling pathway genes including (Wnt mophorgenes: *AXIN2* (p = 0.0405), *CTNNB1* (p = 2.8851E-05), *FGFR1* (p = 0.0061); and FGF morphogenes: *LEF1* (p = 0.0008), *PTK2* (p = 0.0009) and *RhoA* (p = 1.0601E-05)) when compared to the control condition in MDA-MB-231 cells (**Figure 4C & D**). While SDC4KD resulted in fewer changes to Wnt and FGF pathway gene expression, treatment of the cultures induced a significant increase in the gene expression of *CTNNB1* (p = 0.0009), but resulted in a significant decrease in gene expression of *FGFR1* (p =

0.0035) (**Figure 4C & D**).

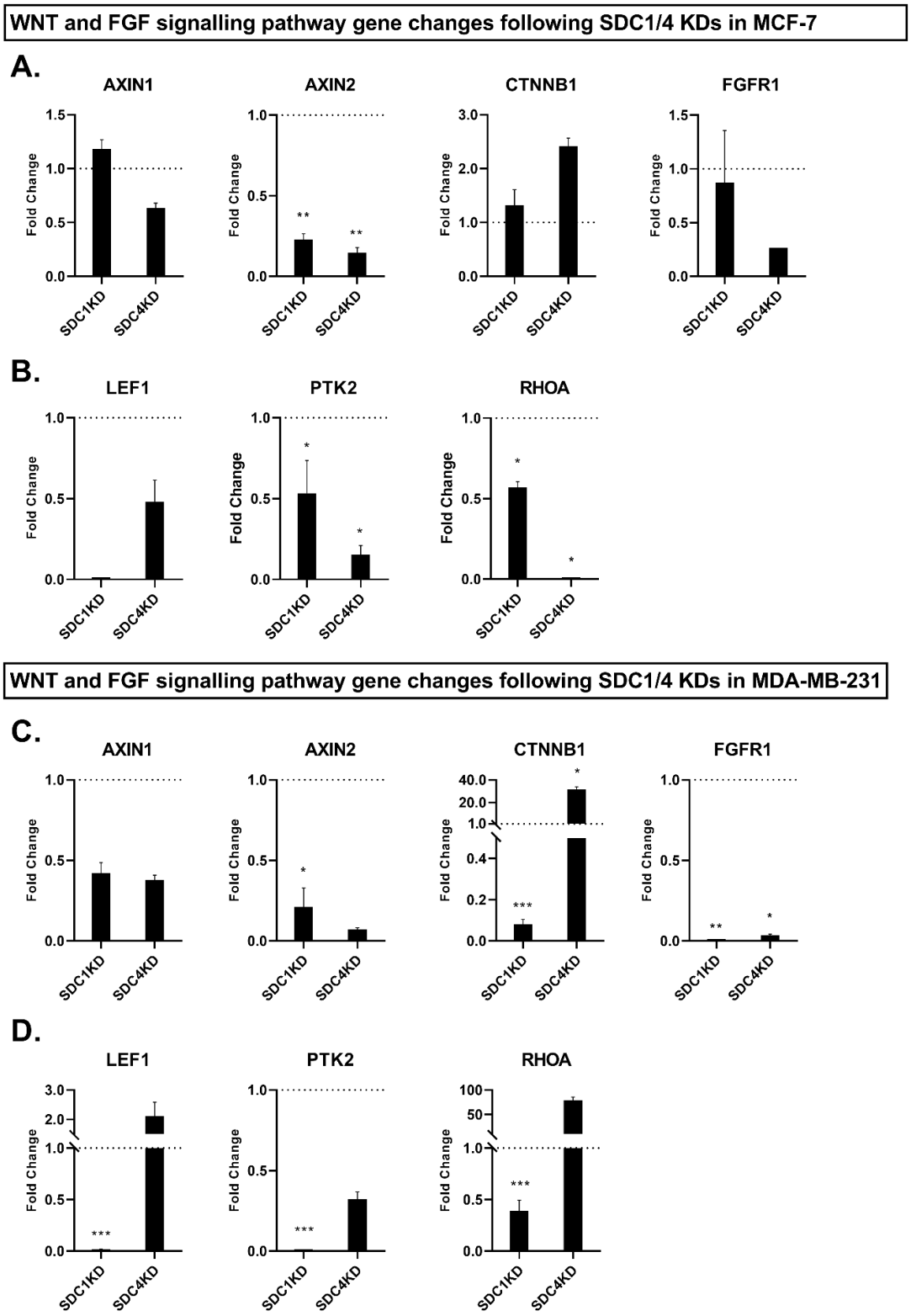

Figure 4. *Changes in gene expression in MCF-7 of (A): Wnt (AXIN 1,2, β-catenin: CTNNB1, fibroblast growth factors: FGFR1) and (B): FGF signalling pathway genes (Lymphoid enhancer-binding factor 1: LEF1, protein tyrosine kinase 2: PTK2, and ras homolog family member A : RHOA); and in MDA-MB-231 cells (C): Wnt and (D): FGF signalling pathway genes post SDC1KD,*

*SDC4KD. SDC1KD decreased the gene expression of both the Wnt and FGF signalling pathways, in both cell lines MCF-7 and MDA-MB-231. The control mean is represented by the dotted line and is set to 1.0 fold change with the standard deviation of the experimental groups represented by the error bars. Each gene expression experiment was perfomed in biological triplicate and technical quatruplicate (n=4). P values were determined using Student t-Test with significance denoted by *p<0.05, **p<0.01, ***p <0.001.*

3.4 The Effect of Syndecan Downregulation on Epithelial Mesenchymal Transition (EMT) Marker Expression:

Next, we examined changes in EMT marker expression following SDC KDs to examine the roles of SDCs in EMT. Overexpression of vimentin (VIM) has been shown to correlate with high metastasic BC [28]. The *VIM* gene was poorly expressed in the control and KD conditions in MCF-7 cells, supporting our previous findings [8]. Moreover, *VIM* gene expression after KDs remained unchanged in SDC1/4 KD conditions when compared to the control culture in MCF-7 cells (**Figure 5A**). In addition, VIM protein was not detected in MCF-7 cultures under either control or KD conditions via WB or ICC (**Figure 5B & C**). In contrast, MDA-MB-231 cells expressed a high level of VIM at both the gene and protein level, corresponding to previous studies demonstrating EMT in the metastasis of a highly invasive BC cells [29, 30]. *VIM* gene expression was significantly decreased after SDC1KD (p = 2.1850E-06), but significantly increased in the SDC4KD condition (p = 0.0005) (**Figure 5D & E**). In addition, WB analysis demonstrated protein expression of VIM was detected in both SDC1KD and SDC4KD in MDA-MB-231 cells. ICC was used to illustrate that the VIM protein was strongly expressed in control and KD conditions. Interestingly, when the normalised fluorescence signal intensity was compared to the control conditions (UT/SCR), VIM protein was found to be slightly decreased following SDC1KD (UT: p = 0.00132, SCR: p = 5.4000E-06) and following SDC4KD when compared to the UT (p = 3.3642E-08) condition in MDA-MB-231 cultures (**Figure 5F**).

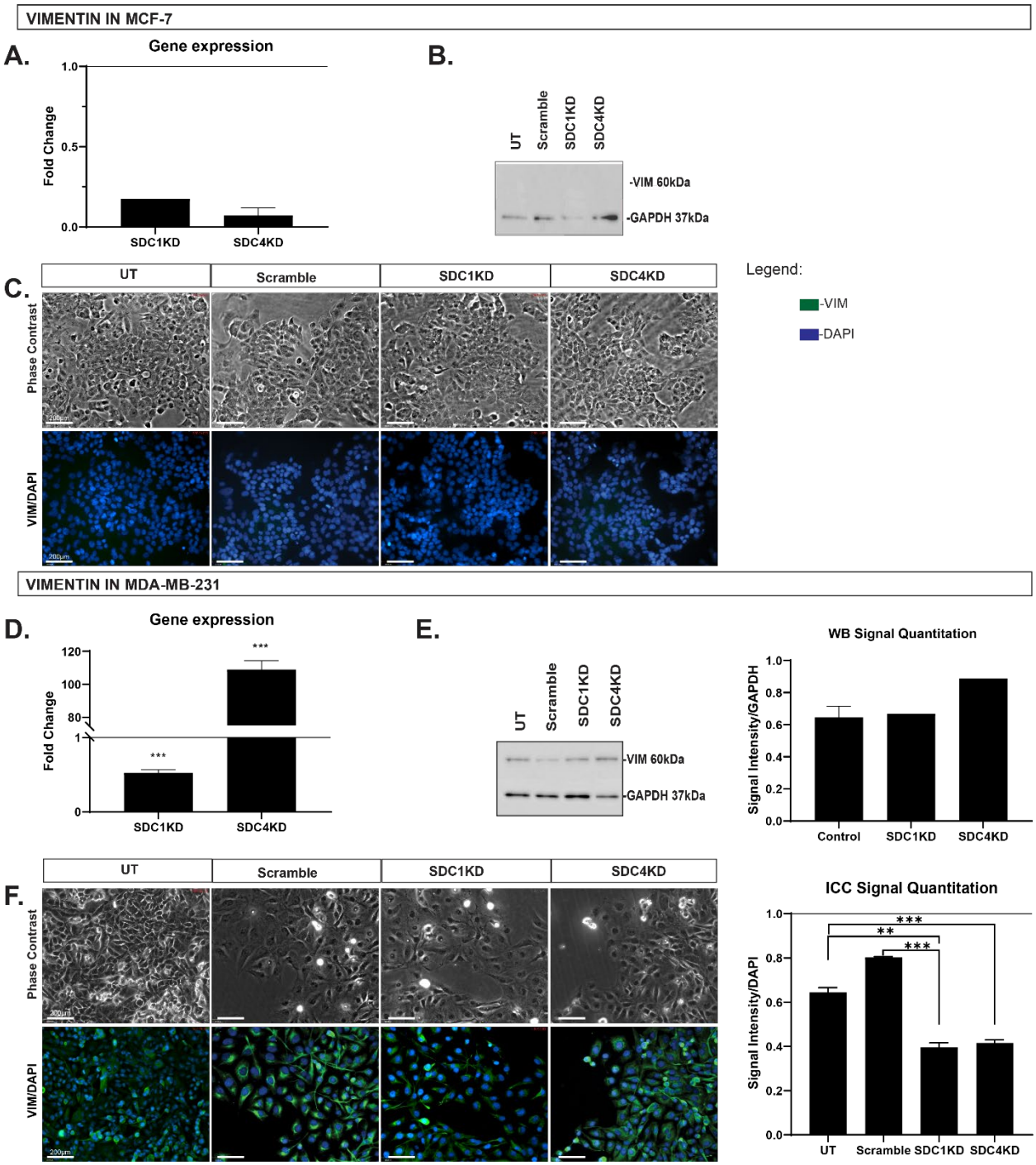

Figure 5. *Epithelial mesenchymal transition marker Vimentin (VIM) post Syndecan (SDC) SDC1 and SDC4 siRNA KDs. In MCF-7 cells: (A) Gene expression of VIM with the control mean represented by the dotted line and is set to 1.0 fold change with the standard deviation of the experimental groups represented by the error bars. Each gene expression experiment was perfomed in biological triplicate and technical quatruplicate (n=4). P values were determined using Student t-Test with significance denoted by *p<0.05, **p<0.01, ***p <0.001, (B) Western analysis of VIM proteins expression at 96 h time point with GAPDH used as the loading control, (C) Immunocytochemistry (ICC) of vimentin (FITC/green) at 96 h time point-counterstained with DAPI (blue; 20 x magnification; scale bar = 200 µm). In MDA-MB-231 cells: (D) Gene expression of VIM, (E) Western analysis of VIM proteins expression, and (F) ICC of vimentin. Signal intensity was Immunofluorescence signal intensity of*

*SDCs as measured by Volocity Cellular Imaging & Analysis software (Perkin Elmer) was normalised to the signal intensity of DAPI. ICC signal intensity difference was examined by ANOVA test with significance denoted by *p<0.05, **p<0.01, ***p <0.001.*

CD44 is also known as the EMT marker, with *CD44* gene expression in MCF-7 cells significantly decreased following HSPG core protein downregulation for SDC1KD (p = 0.0268) (**Figure 6A**). Further investigation into the effects of HSPG core protein KDs on protein expression of CD44 were completed via WB and ICC. CD44 protein was not detected by WB and ICC in MCF-7 cultures (**Figure 6B & C**). In MDA-MB-231 cultures, significant changes to CD44 gene expression was observed following SDC4KD (p = 1.0249E-05) (**Figure 6D**). However, CD44 protein was clearly visible in MDA-MB-231 cells via ICC staining, demonstrating cell-surface localisation in both control and SDC4KD cultures by both WB and ICC (**Figure 6E & F**). CD44 protein was detected in UT, SDC1KD and SDC4KD cultures with levels in SCR cultures almost undetected via WB in MDA-MB-231 cells. CD44 protein showed a visually higher level of expression in SDC4KD cultures when compared to control and SDC1KD cultures in MDA-MB-231 cells via ICC (**Figure 6F**). In addition, the ICC signal intensity was quantitated to normalised to the control (UT/SCR) condition that CD44 protein was decreased in SDC1KD when compared to the control conditions (UT: p = 0.0070, SCR: p = 8.6027E-10), and in SDC4KD when compared to the UT (p = 7.6448E-11) in MDA-MB-231 cells.

In short, both VIM and CD44 gene and protein expression was were not detected in MCF-7 cells, but were highly expressed in the MDA-MB-231 cultues [29-31]. SDC1KD resulted in the downregulation of *VIM* gene expression in MDA-MB-231 cells and in the downregulation of *CD44* in MCF-7 and MDA-MB-231 cultures when compared to the control (UT and SCR). SDC4KD also decreased *VIM* gene and protein expression in MDA-MB-231 cultures.

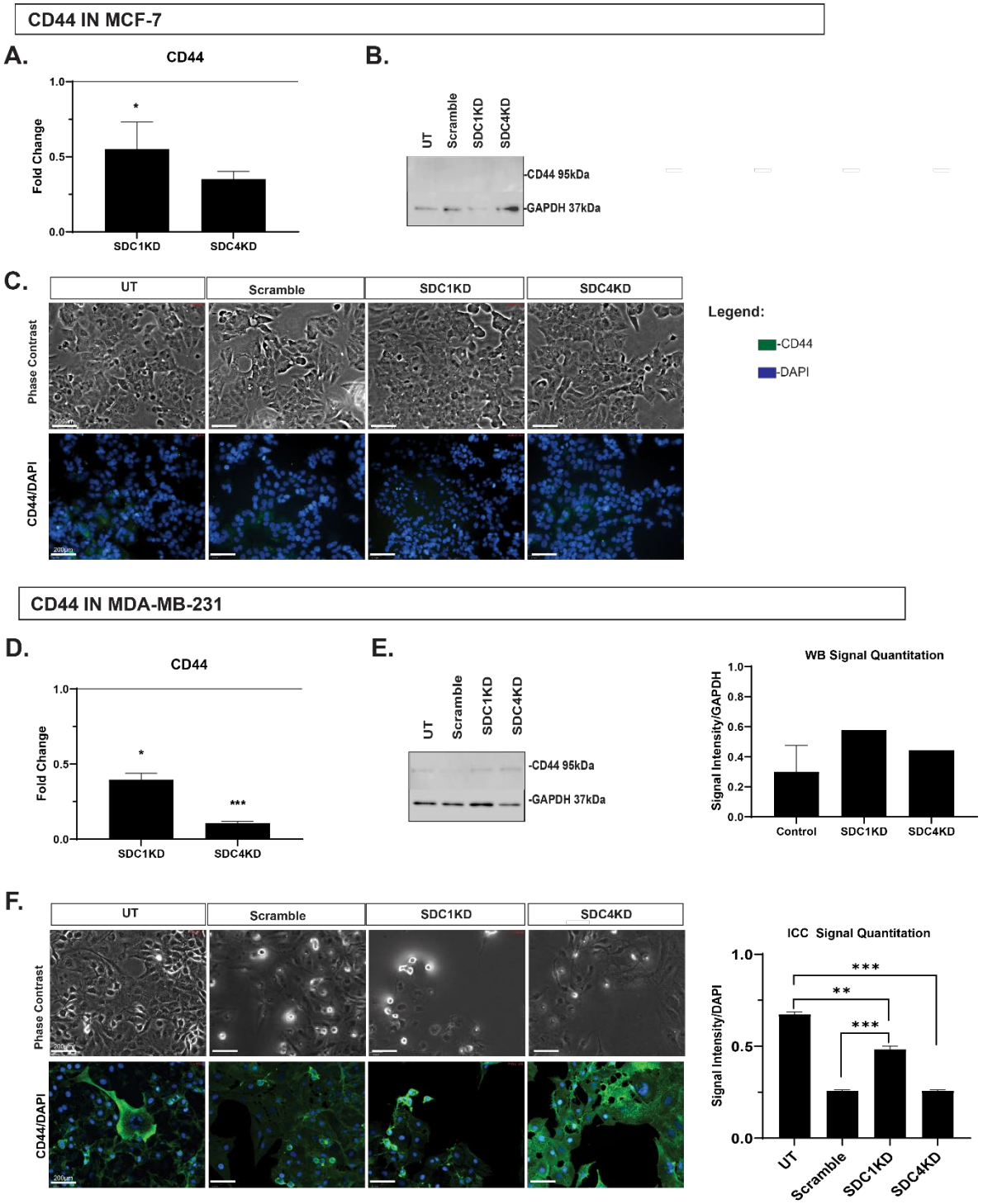

Figure 6. *Epithelial mesenchymal transition marker Indian blood group protein CD44 post Syndecan (SDC1) and SDC4 siRNA KDs. In MCF-7 cells: (A) Gene expression of CD44 with the control mean represented by the dotted line and set to 1.0 fold change with the standard deviation of the experimental groups represented by the error bars. Each gene expression experiment was perfomed in biological triplicate and technical quatruplicate (n=4). P values were determined using Student t-Test with significance denoted by *p<0.05, **p<0.01, ***p <0.001, (B) Western analysis of CD44 protein expression at 96 h time point with GAPDH used as the loading control, (C) Immunocytochemistry (ICC) of CD44 (FITC/green) at 96 h time point-counterstained with DAPI (blue; 20 x magnification; scale bar = 200 μm). In MDA-MB-231 cells: (D) Gene expression of CD44,*

*© Western analysis of CD44 proteins expression, and (F) ICC of CD44. Signal intensity was Immunofluorescence signal intensity of SDCs as measured by Volocity Cellular Imaging & Analysis software (Perkin Elmer) normalised to the signal intensity of DAPI. ICC signal intensity difference was compared using ANOVA and significance denoted by *p<0.05, **p<0.01, ***p <0.001.*

3.5 Effect of Exogenous Heparin and FGF-2 on Cell Migration

To further understand the potential roles of SDCs in mediating BC cell motility, the effects of heparin and FGF-2 treatment on MCF-7 and MDA-MB-231 cell migration were examined. Heparin and FGF-2 are known as the agonist/growth factor that bind to HSPGs and promote cell proliferation and motility [32, 33]. The MCF-7 and MDA-MB-231 cells were grown routinely as a monolayer with variations in serum concentration and growth factors as described. Culturing conditions included 2% FBS, 10% FBS, 2% FBS + 10 μg/mL heparin (hep), 10% FBS + 10 μg/mL hep, 2% FBS + FGF-2 and 10% FBS + FGF-2. To test the effect of the different culturing conditions on cell migration, monolayers were scratched and images were taken at 12/24/48/72 h to monitor migration. Migration was measured by selecting three points (top, middle, bottom) of the scratched area to measure the width of the scratch as previously described (**Figure 7**).

For MCF-7 cells after 72 h, cells grown under 10% FBS control culture demonstrated a higher percentage of wound closure (25%) than cells grown under 2% FBS conditions (18%). The 10% FBS + hep demonstrated the greatest wound closure percentage of all the conditions at approximately 31% (**Figure 7A**). After 48 h the MDA-MB-231 cells exhibited similar wound closure percentages (at 100% closure; **Figure 7B**) despite the variations in FBS, heparin and growth factor concentrations. Interestingly, while MCF-7 cells grown under 2% FBS control conditions (no growth factors) demonstrated the slowest wound closure (17.8%) in most of the culture conditions (**Figure 7C**), MDA-MB-231 cells increased the wound closure percentage (from 3.1% to 94.9%) from 12 h to 24 h in 10% FBS + hep (**Figure 7D**).

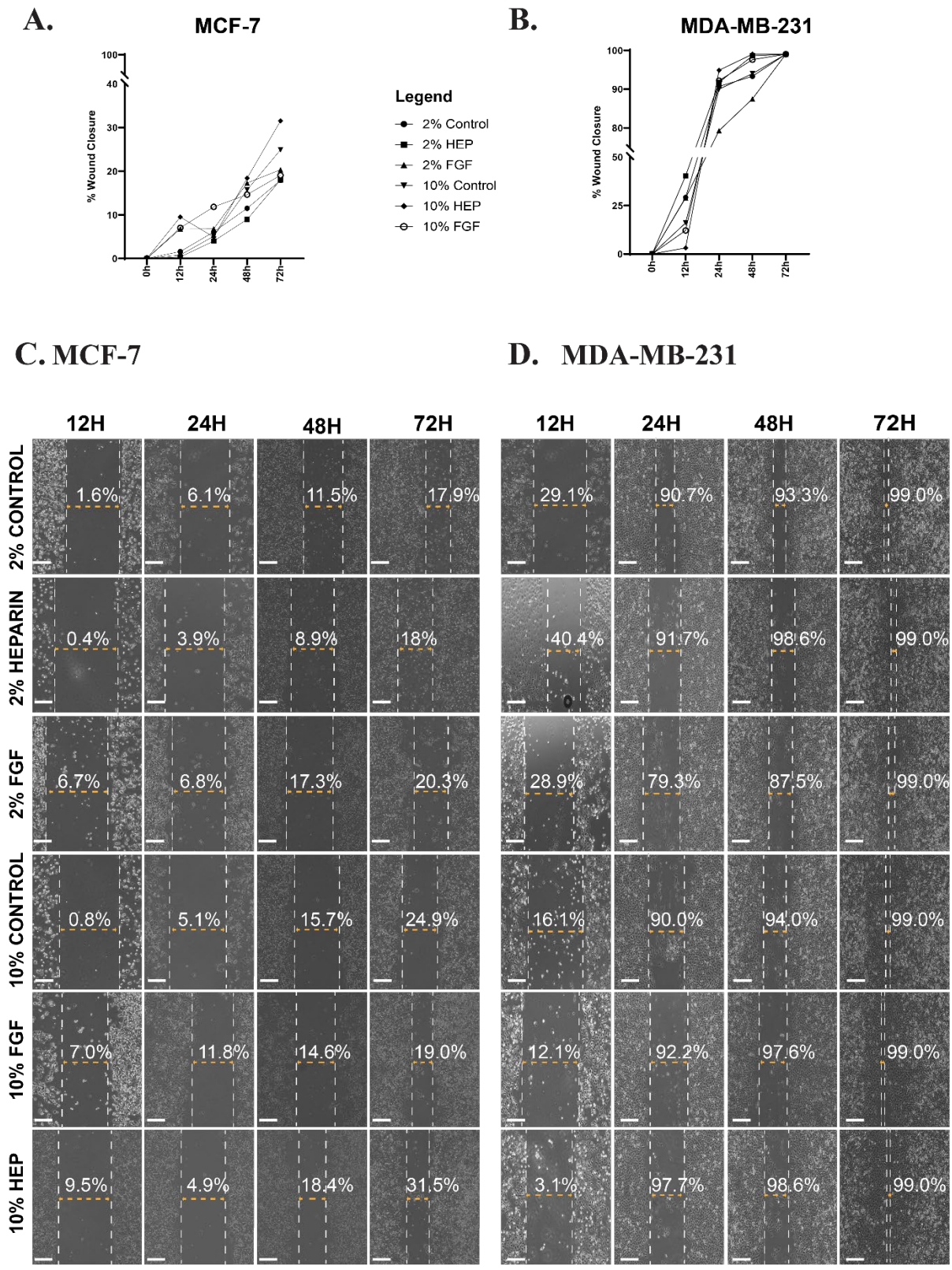

***Figure** 7. The effects of heparin and fibroblast growth factor (FGF) FGF-2 on BC cell migration. The wound clousure percentage were taken in different conditions (2% FBS control, 2% FBS +10 µg/mL heparin, 2% FBS + 10ηg/mL FGF-2, 10% FBS control, 10% FBS + 10 µg/mL heparin, and*

10% FBS + 10ηg/mL FGF-2) at 0h, 12h, 24h, 48h, and 72h in (A) MCF-7, and in (B) MDA-MB-231. The phase contrast images of BC in all cultures at corresponding time points in (C) MCF-7 and (D) MDA-MB-231. Phase contrast images were taken at 4 x magnification, scales bars 100 µM.

In HSPG KD cell cultures, MCF-7 cells grown under the UT and SCR culture conditions demonstrated similar cell migration rates. The migration speed of the SCR condition (14.4%) was slightly faster than the untreated cultures (10.4%) at 72 h in MCF-7 culture (**Figure 8A & C**). In SDC KD cultures MCF-7 cell migration was lower than the rate of the control conditions (UT and SCR), interestingly SDC1KD showed a higher percentage (14.6%) of wound closure than cells under other culture conditions (**Figure 8A**). The percentage of wound closure in the SDC1KD show the highest rate at the period between 24 to 48 h with a roughly 10% increase when compared to other cultures in MCF-7 cells.

In contrast, MDA-MB-231 cells had higher rate of wound closure when compared to the MCF-7 cells in the UT and SCR conditions (**Figure 8B**). However, the wound closure percentage of MDA-MB-231 cells in UT condition exhibited the highest rate, in particular between the 24 to 48 h timepoints. In summary, the SDC1KD showed a higher percentage of wound closure in MCF-7 cells (14.6%), but lower in the MDA-MB-231 cell line (17.9 %) when compared to the UT conditions (MCF-7: 10.4%; MDA-MB-231: 20.5%). Interestingly, SDC4KD showed the lowest rate of cell migration (4.6%) at 72 h in MCF-7, while the SDC4KD condition in MDA-MB-231 cells showed the lowest rate of cell migration (5.8%) after 72 h.

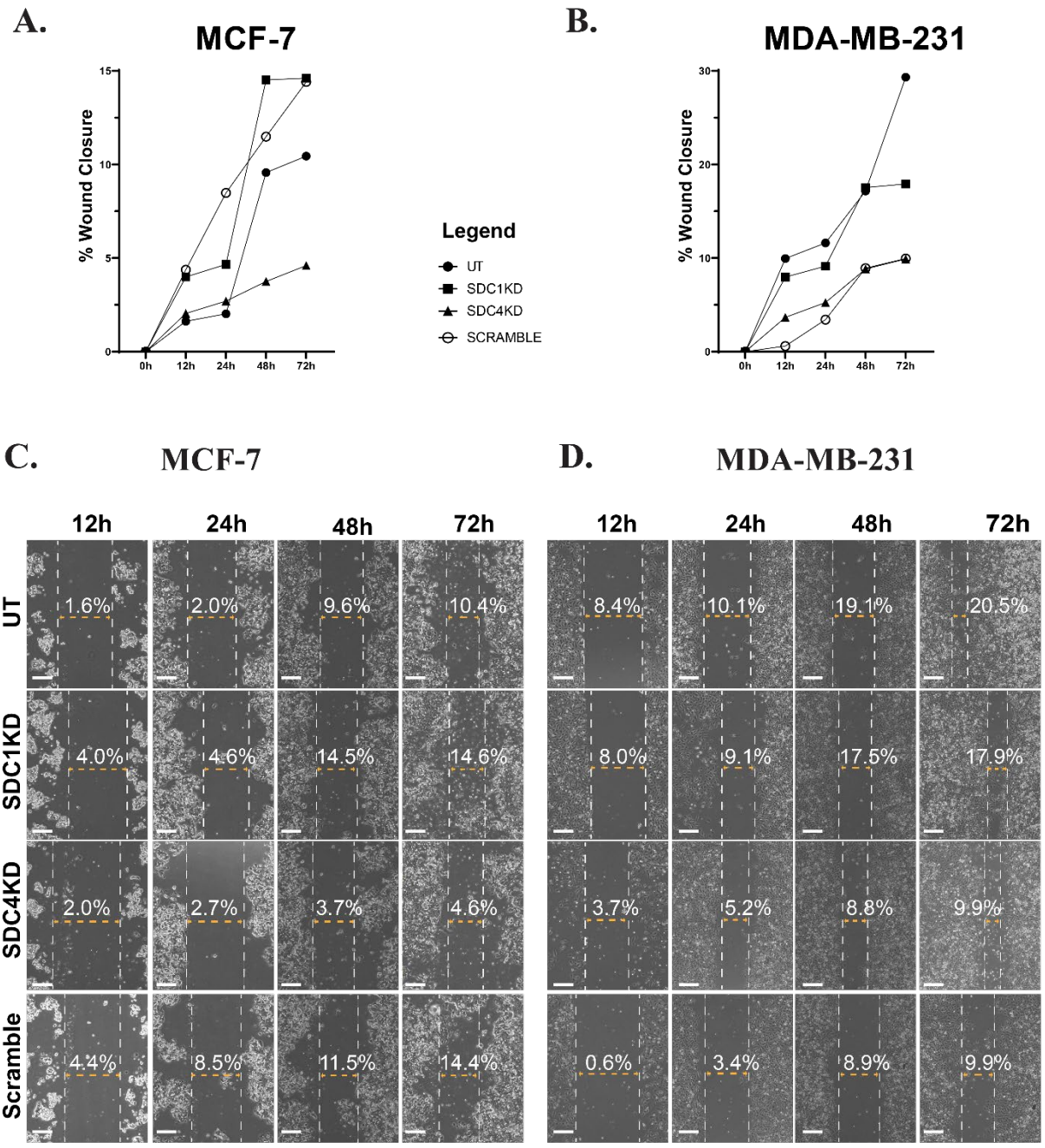

Figure 8. *Effects of heparan sulfate proteoglycan (HSPG) knockdown (KD) cultures on breast cancer (BC) migration. The wound clousure percentage was taken in different conditions (Untreated (UT), SDC1KD, SDC4KD, and Scrambled) at 0 h, 12 h, 24 h, 48 h, and 72 h in (A) MCF-7, and (B) MDA-MB-231 cells. The phase contrast images of BC in all culture conditions at corresponding time points in (C) MCF-7 and (D) MDA-MB-231. Phase contrast images were taken at 4 x magnification, scales bar 100 µM.*

4. Discussion

BC is heterogeneous in nature with thousands of genes involved in its predisposition, initiation

and progression, the deregulation of any of which may contribute to BC pathophysiology through genomic or epigenomic events [34, 35]. In this study, two BC cell lines, MCF-7, a poorly invasive and poorly metastatic, and MDA-MB-231, a highly invasive and highly metastatic human BC cell line, were examined representing contrasting and diverse human BC cell properties. By utilising these two BC cell lines, we determined variations between the two subtypes of BC in gene and protein expression associated with their roles in the ECM and localisation within the microenvironment. Variations in HS chain length and sulfation are known to affect the binding of various growth factors and morphogens [36]. To understand the cell surface protein expression of *SDC1* and *SDC4* in MCF-7 and MDA-MB-231, the gene expression of HSPG core proteins and their associated biosynthetic enzymes as well as Wnt/FGF signalling pathway components were analysed. We also investigated HSPG core proteins in BC by using siRNAs to knockdown specific *SDC1* and *SDC4* genes. Subsequent experiments were conducted to examine how SDC1KD and SDC4KD affected gene expression of other HSPG related genes including other HSPG core proteins (including SDC1-4 and GPC1, -4, -5 and -6) with no significant differences in GPC gene expression observed, suggesting the examined GPCs are not key contributors to these human BC models) and HS biosynthesis enzymes. The analysis of independent experiments showed significant downregulation of SDC1 and SDC4 gene and protein expression under KD conditions in both the MCF-7 and MDA-MB-231 BC cell lines, confirming successful knockdown. The downregulation of SDC genes also affected the expression of Wnt/FGF pathway morphogens, which are associated with cell-cell adhesion and cancer cell differentiation [19, 37]. High expression of SCD1 has previously been corresponded to poor prognosis, while increased expression of *SDC4* has been correlated with better prognosis [38]. Interactions between FGF2/FGFR1 requires the involvement of HSPGs and has been established within the FGF signalling pathway [39], but the exact nature of the co-operation between these morphogens is not well understood. Interestingly, in this study we found that the SDC KDs also decreased the gene expression of some Wnt/FGF morphogenes, which suggests the SDCs regulate these pathways and potentially cell adhesion and differentiation in BC via these signalling pathways [40, 41].

Alterations in gene expression of the HSPG biosynthesis and modification enzymes responsible for the high structural and functional diversity of HSPGs were also examined in this study. HS chains

are synthesised by a complex and temporal process requiring various initiation/elongation (*EXT 1 & 2*), polymerisation (*GCLE*), modification (*NDST1-2*) and sulfation enzymes (*HS2ST1* & *HS6ST1*). Analysis of these biosynthesis enzymes in our KD cultures revealed multiple significant changes following downregulation of specific core proteins. In addition, HSPG biosynthesis and modifications are established mediators of cancer growth [42], thus, changes in these genes by SDC KD suggest the SDCs may regulate cancer progression via these proteins.

SDC1KD significantly increased the gene expression of *GCLE* in MCF-7 cells, but significantly decreased *EXT1*/*2* and *GCLE* in MDA-MB-231 cell culture. This inverse expression pattern of biosynthesis enzymes post SDC1KD suggests that the MCF-7 and MDA-MB-231 cells respond differently to the downregulation of SDC1. Our results showed decreased gene expression following SDC1KD of the elongation enzymes (*EXT1 & 2*) and increased non-significant gene expression level of *GCLE* following SDC4KD in both MCF-7 and MDA-MB-231 cell lines. As an example, SDC1 facilitates binding of FGF-2 to FGFR1 via its HS side chains requiring the action of HS6ST1 [21], which correlates with data obtained in this study with SDC1KD cultures in both cell lines exhibiting decreased HS biosynthesis *EXT1, EXT2, GCLE, NDST1, NDST2* enzyme gene expression; and downregulated *FGFR1* gene expression [21, 43]. SDC4KD also resulted in different changes in biosynthesis and modification enzymes between the two cell lines. In the MDA-MB-231 cell line, following SDC4KD, the majority of the HS biosynthesis and modification enzymes were found to be upregulated (*EXT1* & *-2*, *NDST1* & *-2*, *HS2ST1* and *HS6ST1)*, in contrast to their expression profiles in the MCF-7 cell line. Thus, SDC1 KD differentially affects expression of HS enzymes and may alter the expression of other HSPGs via the regulation of HS biothesis and modification [44]. Data from this study suggests that SDC1 is involved in positive/negative feedback loops in the HS biosynthesis and modification processes, which result in different types and amounts of HS presented at the cell surface or in the microvenviroment surrounding breast cancer cells [45]. The regulation of specific HSPG expression on the cell surface by SDC1 might mediate cell fate in its differentiation, i.e., SDC1 facilitates the osteo-adipogenic balance in human mesenchymal stems cells (hMSCs) during lineage differentiation [26].

SDCs play prominent roles in cell-cell and cell-ECM interactions regulating adhesion, migration, angiogenesis, and proliferation [46]. SDCs have also been reported to have various

functions in pathogenesis, for example, SDC1 has been shown to promote tumorigenesis by regulating adhesion, angiogenesis, and proliferation [2, 9, 47]. Increased gene expression of *SDC1* is correlated with poor prognosis whilst increased gene expression of *SDC4* is correlated with a better prognosis for BC [17, 38]. Both *SDC2* and *SDC3* gene expression remained unchanged in SDC1/4 KD conditions when compared to the control conditions in both cell lines, suggesting these SDCs are expressed and regulated independently. In our models, we demonstrated that, at both gene and protein expression level, SDC1KD resulted in downregulation of *SDC4* expression and SDC4KD resulted in downregulation of *SDC1* expression in both MCF-7 and MDA-MB-231 cell lines. The results contradict previous reports, where increased *SDC1* gene expression was found to be associated with reduced *SDC4* gene expression and vice versa in breast tissue samples [38]. Although SCD1 and -4 are independent indicators in breast carcinomas, a recent study of the four SDCs (SDC1-4) showed that they share 18 binding proteins corresponding to the SDC consensus interactome [48]. This interaction among SDCs may explain the KD effect when we silence the gene expression of *SDC1*/4 in both BC cell lines. At the protein level, expression of SDC1, as demonstrated by ICC, confirmed gene expression findings with a significant downregulation of SDC1 gene expression observed in the SDC4KD sample when compared to the SCR in MCF-7 cells. In MDA-MB-231 cells, KD of both SDCs resulted in lower SDC1 protein when compared to SCR control cultures. Overall, a distinct expression pattern between the gene and protein level of HSPGs was observed and these results highlight a potential key interaction between the SDC1 and SDC4 genes and their high preotein expression levels in MCF-7 and MDA-MB-231 cells. These results suggest SDC1/4 may be key regulators of cellular processes such as cell proliferation and migration in BC.

HSPGs mediate the activity of growth factors and morphogens including FGF and Wnts as well as their receptors (including *FGFR1*). Previous research has found that both the Wnt and FGF signalling pathways regulate key cellular behaviours with increased *FGFR1* expression related to number of receptor genes in various BC cell lines including MCF-7 and MDA-MB-231 cells [18]. HSPG downregulation in our study resulted in multiple downregulatory effects on the Wnt signalling pathway. Interestingly, SDC1KD downregulated the expression of most Wnt signalling pathway genes examined in MDA-MB-231 cells suggesting the important role of SDC1 mediating

the Wnt pathway in these more invasive BC cells [49]. In MCF-7 cells, β-catenin was non-significantly decreased following both *SDC* KDs. However downregulation of β-catenin in MDA-MB-231 cultures was significant following SDC1KD, suggesting SDC1 may mediate the regulation of the canonical Wnt pathway in more aggressive BC subtypes.

Previous research has also shown that downregulation of the Wnt pathway is linked to EMT in BCs charactersed by a loss of *CTNNB1* expression, and gain of *VIM* gene expression [50]. In this study, SDC1KD induced the downregulation of CTNNB1 and VIM gene expression; thus, SDC1 may contribute to cancer metastasis. In addition, SDC1/4 have previously been shown to regulate cell migration via mediating features of cell adhesion [11]. Further, EMT occurs when cells lose cell adhesion and change cell morphology from epithelial cells (having high structural integrity) to mesenchymal cells (existing largely without direct cell-cell contacts and defined cell polarity) [51]. Activation of Wnt leads to activation of EMT, SDC1KD also leads to downregulation of WNT, and enhances the invasiveness of MDA-MB-231 cells as identified in this study.

EMT is a highly coordinated process, which promotes the detachment of the primary tumour and facilitates metastasis [52]. EMT has been associated with aggressive BC subtypes due to increased proliferation, invasiveness, and metastatic potential [52]. MCF-7 cells are a poorly invasive, lowly metastatic cell line that lacks characteristics of EMT, while MDA-MB-231 cells are a highly invasive and highly metastatic cell line possessing characteristics of EMT [34]. The protein expression of VIM, a marker of EMT, was assessed via WB and ICC and found to be low/absent in MCF-7 and significantly higher in MDA-MB-231 cells [53]. Interestingly, SDC1KD downregulated VIM gene expression at the protein level (compared to UT) in MDA-MB-231 cells. With previous work [51] demonstrating activation of EMT via activation of Wnt, the effect of SDC1KD on WNT suggests SDC1 may play a role in BC, potentially via enhancing invasiveness.

The SDC1KD also produced a lower rate of cell migration when compared to the SCR condition in the MCF-7 cells, and to the UT condition in MDA-MB-231 cells, indicating SDC1 could be an important therapeutic target in BC treatment.

Moreover, VIM gene and protein expression levels correlated with aggressive BC subtypes with higher VIM levels detected in the more aggressive BCs (i.e in MDA-MB-231 cells) which correlates with high *SDC1* gene expression as a poor prognostic indicator [17, 38]. In this study, SDC1KD also decreased *VIM* gene expression, supporting this premise and that SDC1 and VIM may interact with each other in the highly invasive MDA-MB-231 cells. However, protein level

analysis of SDC1KD on VIM protein did not correlate with the gene expression data, suggesting that SDC1 and VIM do not interact on the protein level or that alternate regulators influence their gene and protein levels differentially. CD44 protein expression showed a similar expression pattern to VIM in that low expression levels were detected in MCF-7 cultures and high expression was detected in MDA-MB-231 cells. In addition, CD44 protein expression (via both WB and ICC) was significantly decreased in SDC1/4 KD cultures when compared to the UT condition in MDA-MB-231, suggesting SDC1 and CD44 may stimulate each other. SDC1KD also induced a lower migration rate when compare to the UT condition in MDA-MB-231 cultures.

MCF-7 cells are commonly considered to have low metastatic potential, and the cellular migration speed to be slower than MDA-MB-231 cells [54]. Due to their high metastatic potential, MDA-MB-231 cells were able to migrate within 24 h to close the wound, as determined through scratch assays. Despite the high potential for cell metastasis, the addition of heparin and FGF-2 resulted in non-significant changes between these heparin and FGF-2 treated cultures. For the less invasive MCF-7 cells, a higher migration speed was observed in the heparin culture condition when compared to the control culutres, which suggests enhancement of HSPGs increased the migration of MCF-7 cells [55, 56]. These results suggest MCF-7 cells are more responsive to heparin and FGF-2 treatment, with these pathways less important in mediating the MDA-MB-231 cells. In addition, the cell migration characteristics were found to be inhibited in SDC1KD conditions in MDA-MB-231, when compared to the UT conditions. Thus, SDC1 appears to be a mediator of cell migration in the highly invasive MDA-MB-231 BC cell line.

Overall, our data demonstrated *SDC1* and *SDC4* to be highly expressed in both MCF-7 and MDA-MB-231 cells. *SDC1/4* downregulation altered HSPG core proteins and associated biosynthesis and modification enzyme profiles, showing that HSPGs interact not only with each other but also regulate various other biosynthesis enzymes and Wnt pathway component genes. SDC1KD downregulated Wnt and FGF pathway genes in the MDA-MB-231 cell line, highlighting SDC1 may play a key role via the Wnt pathway to mediate proliferation and migration of more aggressive BC. Further analysis into the Wnt/FGF pathway interactions with HSPGs, specifically targeting *SDC1* may provide a new understanding of coordinated interactions and provide an opportunity to target aggressive cancer cells and limit BC progression. In short, SDC1 may become

a potential therapeutic target for BC treatment.

5. Conclusions

SDC involvement in signalling processes predominantly occurs through the sulfation pattern of their HS side chains. Without the combination of sulfation processes of HS chains attached to a core protein enabling specific interactions with relevant ligands to induce or inhibit cell signalling would not be possible. The enzymes that modify these GAG chains, both early in biosynthesis following initiation and polymerisation, and those that continually modify the chains, are of vital importance for tissue and time-specific functions. Alteration of sulfation of these side chains alters the ability of SDCs to interact with cells and the local microenvironment and influence significant downstream effects. In the case of BC, this includes tumour invasiveness, tumour cell proliferation and metastasis of cancer cells. The ability to control the development of a tumour and drive it into a less invasive state would markedly improve patient prognosis.

6. Figure Legends.

Figure 1. The efficiency of heparan sulfate proteoglycans (HSPG) downregulation of syndecan (SDC) *SDC1* and *SDC4* genes following targeted siRNA knockdown (KD) (A) KD efficiency of *SDC1* and *SDC*4 in basal MCF-7 and (B) the MDA-MB-231 cultures. The KD efficiency was examined by gene expression of *SDC1* and *SDC4* in SDC1KD and SDC4KD was compared to control conditions respectively. KD of *SDCs* resulted in significantly decreased gene expression of *SDC1* (MCF-7: 51% with p = 0.0424, MDA-MB-231: 51% with p = 0.0067) and *SDC4* (MCF7: 75% with p = 0.0456, MDA-MB-231: 44% with p = 0.0014) in both cell lines suggesting the gene specific siRNAs provide high efficiency in silencing the target HSPG core proteins. HSPG core protein gene expression profile of (A) MCF-7 and (B) MDA-MB-231 cells following *SDC1* and *SDC4* siRNA KDs. The untreated and scrambled conditions were combined to form the control condition to which gene expression was normalised. Relative gene expression in MCF-7 cells of (C) *SDC1-4* (D) *GPC1,-4* and *-6*; and in MDA-MB-231 cells of (E) *SDC1-4*, (F) glypican (GPC) *GPC1,-5* and *-6*. The control mean is represented by the dotted line and is set to 1.0 fold change with the standard deviation of the experimental groups represented by the error bars. Each gene expression experiment was perfomed in biological triplicate and technical quatruplicate (n=4). P values were determined using Student t-Test with significance denoted by *p<0.05, **p<0.01, ***p <0.001.

Figure 2. Immunocytochemistry (ICC) of syndecan (SDC) SDC1 and SDC4 following *SDC1/4* siRNA knockdowns: SDC1 (FITC/green) and SDC4 (Cy3/yellow) detected at 96 h time point in (A) MCF-7 and (B) MDA-MB-231 cells– counterstained with DAPI (blue; 40X magnification, scale bar 200 μm). Immunofluorescence signal intensity of SDCs as measured by Volocity Cellular Imaging & Analysis software (Perkin Elmer) was normalised to the signal intensity of DAPI. SDC1 and SDC4 protein expression compared to DAPI were higher in MDA-MB-231 cells when compared to MCF-7 cells with distinctly different localisation patterns: SDC1 localisation was more ubiquitous throughout the MDA-MB-231 cells while SDC4 localised around the nucleus in cluster formations. The SDC knockdown (KD) SDC1KD and SDC4KD conditions showed reduced protein expression of SDC1 and SDC4 in both MCF-7 and MDA-MB-231 cells compared to the scramble controls. ICC signal intensity difference was determined by ANOVA with significance denoted by *p<0.05, **p<0.01, ***p <0.001.

Figure 3. Relative Gene Expression of heparan sulfate (HS) chain initiation and modification enzymes following syndecan (SDC) *SDC1* and *SDC4* siRNA knockdown (KD): (A) Exostoses (*EXT1 & 2*), (B) C5-Epimerase (*GCLE*), (C) N-deacetylase/N-sulfotransferases (*NDST1 & NDST2*), (D) 2-O/6-O-sulfotransferases (*HS2ST2 & HS6ST1*); and in the MDA-MB-231 cell lines: (E) *EXT1 & 2*, (F) *GCLE*, (G) *NDST1 & NDST2*, (H) *HS2ST2 & HS6ST1*. The knockdown of *SDC1/4* induced significant changes in gene expression of HS chain initiation and modification enzymes in both cell lines. The control mean is represented by the dotted line and is set to 1.0 fold change with the standard deviation of the experimental groups represented by the error bars. Each

gene expression experiment was perfomed in biological triplicate and technical quatruplicate (n=4). P values were determined using Student t-Test with significance denoted by *p<0.05, **p<0.01, ***p <0.001.

Figure 4. Changes in gene expression in MCF-7 of (A): Wnt (*AXIN 1,2*, β-catenin: *CTNNB1*, fibroblast growth factors: *FGFR1*) and (B): FGF signalling pathway genes (Lymphoid enhancer-binding factor 1: *LEF1*, protein tyrosine kinase 2: *PTK2*, and ras homolog family member A : *RHOA*); and in MDA-MB-231 cells (C): Wnt and (D): FGF signalling pathway genes post SDC1KD, SDC4KD. SDC1KD decreased the gene expression of both the Wnt and FGF signalling pathways, in both cell lines MCF-7 and MDA-MB-231. The control mean is represented by the dotted line and is set to 1.0 fold change with the standard deviation of the experimental groups represented by the error bars. Each gene expression experiment was perfomed in biological triplicate and technical quatruplicate (n=4). P values were determined using Student t-Test with significance denoted by *p<0.05, **p<0.01, ***p <0.001.

Figure 5. Epithelial mesenchymal transition marker Vimentin (VIM) post Syndecan (SDC) *SDC1* and *SDC4* siRNA KDs. In MCF-7 cells: (A) Gene expression of *VIM* with the control mean represented by the dotted line and is set to 1.0 fold change with the standard deviation of the experimental groups represented by the error bars. Each gene expression experiment was perfomed in biological triplicate and technical quatruplicate (n=4). P values were determined using Student t-Test with significance denoted by *p<0.05, **p<0.01, ***p <0.001, (B) Western analysis of VIM proteins expression at 96 h time point with GAPDH used as the loading control, (C) Immunocytochemistry (ICC) of vimentin (FITC/green) at 96 h time point-counterstained with DAPI (blue; 20 x magnification; scale bar = 200 μm). In MDA-MB-231 cells: (D) Gene expression of *VIM*,

(E) Western analysis of VIM proteins expression, and (F) ICC of vimentin. Signal intensity was Immunofluorescence signal intensity of SDCs as measured by Volocity Cellular Imaging & Analysis software (Perkin Elmer) was normalised to the signal intensity of DAPI. ICC signal intensity difference was examined by ANOVA test with significance denoted by *p<0.05, **p<0.01, ***p <0.001.

Figure 6. Epithelial mesenchymal transition marker Indian blood group protein (CD44) post Syndecan (SDC1) and SDC4 siRNA KDs. In MCF-7 cells: (A) Gene expression of *CD44* with the control mean represented by the dotted line and set to 1.0 fold change with the standard deviation of the experimental groups represented by the error bars. Each gene expression experiment was perfomed in biological triplicate and technical quatruplicate (n=4). P values were determined using Student t-Test with significance denoted by *p<0.05, **p<0.01, ***p <0.001, (B) Western analysis of CD44 protein expression at 96 h time point with GAPDH used as the loading control, (C) Immunocytochemistry (ICC) of CD44 (FITC/green) at 96 h time point-counterstained with DAPI

(blue; 20 x magnification; scale bar = 200 μm). In MDA-MB-231 cells: (D) Gene expression of *CD44*, (E) Western analysis of CD44 proteins expression, and (F) ICC of CD44. Signal intensity was Immunofluorescence signal intensity of SDCs as measured by Volocity Cellular Imaging & Analysis software (Perkin Elmer) normalised to the signal intensity of DAPI. ICC signal intensity difference was compared using ANOVA and significance denoted by *p<0.05, **p<0.01, ***p <0.001.

Figure 7. The effects of heparin and fibroblast growth factor (FGF) FGF-2 on BC cell migration. The wound clousure percentage were taken in different conditions (2% FBS control, 2% FBS +10 μg/mL heparin, 2% FBS + 10ηg/mL FGF-2, 10% FBS control, 10% FBS + 10 μg/mL heparin, and 10% FBS + 10ηg/mL FGF-2) at 0h, 12h, 24h, 48h, and 72h in (A) MCF-7, and in (B) MDA-MB-231. The phase contrast images of BC in all cultures at corresponding time points in (C) MCF-7 and (D) MDA-MB-231. Phase contrast images were taken at 4 x magnification, scales bars 100 μM.

Figure 8. Effects of heparan sulfate proteoglycan (HSPG) knockdown (KD) cultures on breast cancer (BC) migration. The wound clousure percentage was taken in different conditions (Untreated (UT), SDC1KD, SDC4KD, and Scrambled) at 0 h, 12 h, 24 h, 48 h, and 72 h in (A) MCF-7, and (B) MDA-MB-231 cells. The phase contrast images of BC in all culture conditions at corresponding time points in (C) MCF-7 and (D) MDA-MB-231. Phase contrast images were taken at 4 x magnification, scales bar 100 μM.

Supplementary Materials:

Supplementary Table 1. siRNA Sequences

Supplementary Table 2: Primer Sequences

Author Contributions:

LMH conceived of and supervised the project, provided funding support, revised and approved the final manuscript. SHP and KP optimised technical details and performed the experiments as well as appropriate data analysis. RKO and LRG provided supervision and technical advice, revised and approved the final manuscript. LEO, CY, IWP, KMTA, MG and TAC assisted with experimental and technical details, revised and approved the final manuscript.

Supplementary

Supplementary Table 1. siRNA Sequences

Accell siRNA		**Sequences**
Scramble	siRNA-1	UGGUUUACAUGUCGACUAA
	siRNA-2	UGGUUUACAUGUUUUCUGA
	siRNA-3	UGUUUACAUGUUUUCCUA
	siRNA-4	UGGUUUACAUGUUGUGUGA
SDC1	siRNA-1	UGCUUAUUUGACAACGUUU
	siRNA-2	CUCUAGUUCUUUGUUCAUA
	siRNA-3	GUGUUGUCUCUUGAGUUUG
	siRNA-4	GGUUCAGCCAAGGUUUUAU
SDC4	SiRNA-1	CCUUGGUGCCUCUAGAUAA
	siRNA-2	GCAACAUCUUUCACACAAC
	siRNA-3	CUGCUAACUUUCUAUUUAA
	siRNA-4	CCUUUCUGCAGAGUGUAUA

Supplementary Table 2: Primer Sequences

Gene	**Forward Primer** 5’ 3’	**Reverse Primer** 5’ 3’	**Ref Sequence (GenBank)**
NDST1	TGGTCTTGGATGGCAAACTG	CGCCAAGGTTTTGTGGTAGTC	NM_00153
NDST2	CCTATTTGAAAAAAGTGCCACCTACT	GCAGGGTTGGTGAGCACTGT	NM_003635
EXT1	TGACAGAGACAACACCGAGTATGA	GCAAAGCCTCCAGGAATCTGAAG	NM_000127.2
EXT2	CAGTCAATTAAAGCCATTGCCCTG	GGGATCAGCGGGAGGAAGAG	NM_000401
C5-Epimerase	AGCTGTCAAGCCAACCAAAATAA	CTTACTAGCCAATCACTAGCAGCAA	AY635582

HST2ST1	TCCCGCTCGAAGCTAGAAAG	CGAGGGCCATCCATTGTATG	NM_012262
HS6ST1	TCTGGAAAGTGCCAAGTCAAATC	GCGTAGTCGTACAGCTGCATGT	NM_004807
SDC1	CTGGGCTGGAATCAGGAATATTT	CCCATTGGATTAAGTAGAGTTTTGC	BC008765.2
SDC2	AGCTGACAACATCTCGACCACTT	GCGTCGTGGTTTCCACTTTT	NM_002998.3
SDC3	CTTGGTCACACTGCTCATCTATCG	GCATAGAACTCCTCCTGCTTGTC	AF248634
SDC4	CCACGTTTCTAGAGGCGTCACT	CTGTCCAACAGATGGACATGCT	BC030805.1
GPC1	GGACATCACCAAGCCGGACAT	GTCCACGTCGTTGCCGTTGT	NM_002081
GPC2	TGATCAGCCCCAACAGAGAAA	CCACTTCCAACTTCCTTCAAACC	NM_152742
GPC4	GGTGAACTCCCAGTACCACTTTACA	GCTTCAGCTGCTCCGTATACTTG	NM_001448
GPC5	GCTCACCTCAATGGACAAAAATT	GTTGGCAAGCGTCTCTTCACT	NM_004466
GPC6	CAGCCTGTGTTAAGCTGAGGTT	GATGTGTGTGCGTGGAGGTATGT	NM_005708
AXIN1	ACAGGATCCGTAAGCAGCAC	GGTACGTGCGGGGAATGT	NM_003502.3
AXIN2	TAACCCCTCAGAGCGATGGA	CCTCCTCTCTTTTACAGCAGGG	NM_004655.3
RHOA	CGTTAGTCCACGGTCTGGTC-	GCCATTGCTCAGGCAACGAA	NM_001313941.1
LEF1	TGCATCAGGTACAGGTCCAAG	ACGTTGGGAATGAGCTTCGT	NM_001098209
CTNNB1	GACGGAGGAAGGTCTGAGGA	AAATACCCTCAGGGGAACAGG	NM_001098209.1
VIM	GGACCAGCTAAGCAACGACAAAA	CGCATTGTGAACATCCTGTCTG	NM_003380.3
CD44	GTGGTTTGGCAACAGATGGC	GAGGCTGCAGCTGTCCC	NM_000610.3
PTK2	TGGGCGGAAAGAAATCCTGC	GGCTTGACACCCTCGTTGTA	NM_001199649.1

FGFR1	TCAGATGCTCTCCCCTCCTC	GAGCTACGGGCATACGGTTT	NM_001174063.1

7. References

1. Cancer Australia, A.G. *Breast cancer in Australia statistics*. 2019; Available from: https://breast-cancer.canceraustralia.gov.au/statistics#:~:text=In%202019%2C%20it%20is%20estimated,and%201%20in%207%20females.
2. Maeda, T., C.M. Alexander, and A. Friedl, *Induction of syndecan-1 expression in stromal fibroblasts promotes proliferation of human breast cancer cells.* Cancer Res, 2004. **64**(2): p. 612-21.
3. Najafi, M., B. Farhood, and K. Mortezaee, *Extracellular matrix (ECM) stiffness and degradation as cancer drivers.* Journal of cellular biochemistry, 2019. **120**(3): p. 2782-2790.
4. Fuster, M.M. and J.D. Esko, *The sweet and sour of cancer: glycans as novel therapeutic targets.* Nat Rev Cancer, 2005. **5**(7): p. 526-42.
5. Yoneda, A., et al., *Breast and ovarian cancers: a survey and possible roles for the cell surface heparan sulfate proteoglycans.* J Histochem Cytochem, 2012. **60**(1): p. 9-21.
6. Fico, A., et al., *Modulating Glypican4 Suppresses Tumorigenicity of Embryonic Stem Cells While Preserving Self-Renewal and Pluripotency.* Stem Cells, 2012. **30**(9): p. 1863-1874.
7. Theocharis, A.D., et al., *Proteoglycans in health and disease: novel roles for proteoglycans in malignancy and their pharmacological targeting.* Febs Journal, 2010. **277**(19): p. 3904-3923.
8. Okolicsanyi, R.K., et al., *Heparan sulfate proteoglycans and human breast cancer epithelial cell tumorigenicity.* J Cell Biochem, 2014. **115**(5): p. 967-76.
9. Burbach, B.J., Y. Ji, and A.C. Rapraeger, *Syndecan-1 ectodomain regulates matrix-dependent signaling in human breast carcinoma cells.* Exp Cell Res, 2004. **300**(1): p. 234-47.
10. Kirn-Safran, C., M.C. Farach-Carson, and D.D. Carson, *Multifunctionality of extracellular and cell surface heparan sulfate proteoglycans.* Cell Mol Life Sci, 2009. **66**(21): p. 3421-34.
11. Baba, F., et al., *Syndecan-1 and syndecan-4 are overexpressed in an estrogen receptor-negative, highly proliferative breast carcinoma subtype.* Breast Cancer Res Treat, 2006. **98**(1): p. 91-8.
12. Ibrahim, S.A., et al., *Syndecan-1 (CD138) modulates triple-negative breast cancer stem cell properties via regulation of LRP-6 and IL-6-mediated STAT3 signaling.* PLoS One, 2013. **8**(12): p. e85737.
13. Onyeisi, J.O.S., C.C. Lopes, and M. Götte, *Syndecan-4 as a Pathogenesis Factor and Therapeutic Target in Cancer.* Biomolecules, 2021. **11**(4).
14. Nikolova, V., et al., *Differential roles for membrane-bound and soluble syndecan-1 (CD138) in breast cancer progression.* Carcinogenesis, 2009. **30**(3): p. 397-407.

15. Li, N., M.R. Spetz, and M. Ho, *The Role of Glypicans in Cancer Progression and Therapy.* J Histochem Cytochem, 2020. **68**(12): p. 841-862.
16. Duplancic, R., et al., *Syndecans and enzymes for heparan sulfate biosynthesis and modification differentially correlate with presence of inflammatory infiltrate in periodontitis.* Frontiers in physiology, 2019. **10**: p. 1248.
17. Barbareschi, M., et al., *High syndecan-1 expression in breast carcinoma is related to an aggressive phenotype and to poorer prognosis.* Cancer: Interdisciplinary International Journal of the American Cancer Society, 2003. **98**(3): p. 474-483.
18. Brady, N.J., Chuntova, P., Bade, L. K., & Schwertfeger, K. L. , *The FGF/FGF receptor axis as a therapeutic target in breast cancer.* . Expert review of endocrinology & metabolism, 2013.
19. Reya, T. and H. Clevers, *Wnt signalling in stem cells and cancer.* Nature, 2005. **434**(7035): p. 843-50.
20. Tkachenko, E., J.M. Rhodes, and M. Simons, *Syndecans: new kids on the signaling block.* Circ Res, 2005. **96**(5): p. 488-500.
21. Nawroth, R., et al., *Extracellular sulfatases, elements of the Wnt signaling pathway, positively regulate growth and tumorigenicity of human pancreatic cancer cells.* PLoS One, 2007. **2**(4): p. e392.
22. Wang, Y. and B.P. Zhou, *Epithelial-mesenchymal transition in breast cancer progression and metastasis.* Chin J Cancer, 2011. **30**(9): p. 603-11.
23. Liu, C.Y., et al., *Vimentin contributes to epithelial-mesenchymal transition cancer cell mechanics by mediating cytoskeletal organization and focal adhesion maturation.* Oncotarget, 2015. **6**(18): p. 15966-83.
24. Morath, I., T.N. Hartmann, and V. Orian-Rousseau, *CD44: More than a mere stem cell marker.* Int J Biochem Cell Biol, 2016. **81**(Pt A): p. 166-173.
25. Oikari, L.E., et al., *HSPGs glypican-1 and glypican-4 are human neuronal proteins characteristic of different neural phenotypes.* J Neurosci Res, 2020. **98**(8): p. 1619-1645.
26. Yu, C., et al., *Syndecan-1 Facilitates the Human Mesenchymal Stem Cell Osteo-Adipogenic Balance.* Int J Mol Sci, 2020. **21**(11).
27. Pinto, B.I., et al., *In Vitro Scratch Assay to Demonstrate Effects of Arsenic on Skin Cell Migration.* J Vis Exp, 2019(144).
28. Serrano, M.J., et al., *EMT and EGFR in CTCs cytokeratin negative non-metastatic breast cancer.* Oncotarget, 2014. **5**(17): p. 7486-97.
29. McInroy, L. and A. Maatta, *Down-regulation of vimentin expression inhibits carcinoma cell migration and adhesion.* Biochem Biophys Res Commun, 2007. **360**(1): p. 109-14.
30. Messica, Y., et al., *The role of Vimentin in Regulating Cell Invasive Migration in Dense Cultures of Breast Carcinoma Cells.* Nano Lett, 2017. **17**(11): p. 6941-6948.
31. Louderbough, J.M. and J.A. Schroeder, *Understanding the dual nature of CD44 in breast cancer progression.* Molecular Cancer Research, 2011. **9**(12): p. 1573-1586.

32. Su, G., et al., *Shedding of syndecan-1 by stromal fibroblasts stimulates human breast cancer cell proliferation via FGF2 activation.* J Biol Chem, 2007. **282**(20): p. 14906-15.
33. Yang, N., et al., *Syndecan-1 in breast cancer stroma fibroblasts regulates extracellular matrix fiber organization and carcinoma cell motility.* Am J Pathol, 2011. **178**(1): p. 325-35.
34. Neve, R.M., et al., *A collection of breast cancer cell lines for the study of functionally distinct cancer subtypes.* Cancer Cell, 2006. **10**(6): p. 515-27.
35. Nguyen, T.L., et al., *Syndecan-1 Overexpression Is Associated With Nonluminal Subtypes and Poor Prognosis in Advanced Breast Cancer.* American Journal of Clinical Pathology, 2013. **140**(4): p. 468-474.
36. Turner, N. and R. Grose, *Fibroblast growth factor signalling: from development to cancer.* Nat Rev Cancer, 2010. **10**(2): p. 116-29.
37. Villegas, S.N., M. Canham, and J.M. Brickman, *FGF signalling as a mediator of lineage transitions--evidence from embryonic stem cell differentiation.* J Cell Biochem, 2010. **110**(1): p. 10-20.
38. Lendorf, M.E., et al., *Syndecan-1 and syndecan-4 are independent indicators in breast carcinoma.* J Histochem Cytochem, 2011. **59**(6): p. 615-29.
39. Mundhenke, C., et al., *Heparan sulfate proteoglycans as regulators of fibroblast growth factor-2 receptor binding in breast carcinomas.* American Journal of Pathology, 2002. **160**(1): p. 185-194.
40. F.Fallon, G., *Fibroblast Growth Factors as Multifunctional Signaling Factors.* 1998.
41. Goolam, M. and M. Zernicka-Goetz, *The chromatin modifier Satb1 regulates cell fate through Fgf signalling in the early mouse embryo.* Development, 2017. **144**(8): p. 1450-1461.
42. Fuster, M.M. and L.C. Wang, *Endothelial Heparan Sulfate in Angiogenesis.* Glycosaminoglycans in Development, Health and Disease, 2010. **93**: p. 179-212.
43. Mali, M., Elenius, K., Miettinen, H. M., & Jalkanen, M. , *Inhibition of basic fibroblast growth factor-induced growth promotion by overexpression of syndecan-1.* Journal of Biological Chemistry, 1993.
44. Carlsson, P. and L. Kjellen, *Heparin biosynthesis.* Handb Exp Pharmacol, 2012(207): p. 23-41.
45. Kreuger, J. and L. Kjellen, *Heparan sulfate biosynthesis: regulation and variability.* J Histochem Cytochem, 2012. **60**(12): p. 898-907.
46. Couchman, J.R., et al., *Fell-Muir Lecture: Syndecans: from peripheral coreceptors to mainstream regulators of cell behaviour.* Int J Exp Pathol, 2015. **96**(1): p. 1-10.
47. Beauvais, D.M. and A.C. Rapraeger, *Syndecan-1-mediated cell spreading requires signaling by alphavbeta3 integrins in human breast carcinoma cells.* Exp Cell Res, 2003. **286**(2): p. 219-32.
48. Gondelaud, F. and S. Ricard-Blum, *Structures and interactions of syndecans.* FEBS J, 2019. **286**(15): p. 2994-3007.
49. Liao, S., et al., *Relationship between SDC1 and cadherin signalling activation in cancer.* Pathol Res Pract, 2020. **216**(1): p. 152756.

50. Thiery, J.P., et al., *Epithelial-mesenchymal transitions in development and disease.* Cell, 2009. **139**(5): p. 871-90.
51. Radisky, D.C., *Epithelial-mesenchymal transition.* Journal of cell science, 2005. **118**(19): p. 4325-4326.
52. Nikitovic, D., et al., *The motile breast cancer phenotype roles of proteoglycans/glycosaminoglycans.* Biomed Res Int, 2014. **2014**: p. 124321.
53. Trogden, K.P., et al., *An image-based small-molecule screen identifies vimentin as a pharmacologically relevant target of simvastatin in cancer cells.* FASEB J, 2018. **32**(5): p. 2841-2854.
54. Farshad H. Shirazi1, e.a., *Remarks in Successful Cellular*
Investigations for Fighting Breast Cancer
Using Novel Synthetic Compounds. 2011: p. 85-102.
55. Johnson, N.R. and Y. Wang, *Controlled delivery of heparin-binding EGF-like growth factor yields fast and comprehensive wound healing.* J Control Release, 2013. **166**(2): p. 124-9.
56. Sun, H., et al., *Development of low molecular weight heparin based nanoparticles for metastatic breast cancer therapy.* Int J Biol Macromol, 2018. **112**: p. 343-355.